Mathematical Biosciences and Engineering

http://www.aimspress.com/journal/mbe

MBE, 23(1): 40–75.
DOI: 10.3934/mbe.2026003
Received: 26 August 2025
Revised: 09 October 2025
Accepted: 22 October 2025
Published: 28 November 2025

Research article

Mathematical modeling of the 2023 dengue outbreak in the Centre Region of Burkina Faso: Parameter estimation and assessment of control strategies

Haoua Tinde[1], **Wenddabo Olivier Sawadogo**[1,2,*], **Pegdwindé Ousséni Fabrice Ouedraogo**[1,3] **and Adama Kiemtore**[1]

[1] Department of Mathematics, Université Joseph Ki Zerbo, 03 BP 7021, Ouagadougou, Burkina Faso
[2] Department of Mathematics and Informatics, Université Lédéa Bernard Ouédraogo, 01 BP 346, Ouahigouya, Burkina Faso
[3] Department of Mathematics, Université Thomas Sankara, 12 BP 417, Ouagadougou, Burkina Faso

* **Correspondence:** Email: wenddabo81@gmail.com.

Abstract: Mathematical models are valuable tools in the fight against infectious diseases such as dengue. However, their use to guide public health strategies in sub-Saharan Africa, particularly in Burkina Faso, remains limited due to the scarcity of locally calibrated models. Moreover, no study has yet applied the African vulture optimization algorithm (AVOA) for dengue parameters in this context. In this study, we develop a compartmental model to evaluate the impact of control strategies on the 2023 dengue epidemic in the Centre Region of Burkina Faso. The model combines a susceptible–infected (SI) structure for the mosquitoes aquatic phase, a susceptible–exposed–infected (SEI) structure for adult mosquitoes, and a susceptible–exposed–infected–recovered (SEIR) framework for the human population. It incorporates key features, including vertical transmission in mosquitoes and a distinction between clinically detected and undetected human cases. After mathematical analysis, key epidemiological parameters were estimated by calibrating the model against weekly reported case data from June to December 2023 using AVOA. The basic reproduction number ($\mathcal{R}_0$) was estimated at 2.30, confirming the potential for sustained transmission. Sensitivity analysis identified the mosquito biting rate (b), larval carrying capacity (k_A), mosquito mortality (μ_V), and the recovery rate of undetected cases as the most influential parameters. Finally, numerical simulations assessed the impact of control measures recommended by the Ministry of Health of Burkina Faso. The results show that the effectiveness of dengue control strategies depends critically on their intensity and, most importantly, their duration, highlighting the need for integrated, intensive, and sustained vector control measures combined with individual protective actions for effective and long-term management of dengue transmission.

Keywords: mathematical modeling; numerical simulation; dengue; parameter estimation; metaheuristics; public health control strategies

1. Introduction

Dengue is a tropical disease transmitted by *Aedes aegypti* and *Aedes albopictus*, primarily affecting urban and semi-urban areas. It has four serotypes (DENV-1 to DENV-4) and represents a growing public health threat in over 100 countries. According to the World Health Organization (WHO), dengue cases increased 10 fold between 2000 and 2019 and exceeded 5 million in 2023, with Burkina Faso particularly affected, recording 146,878 suspected cases and 688 deaths [1].

Mathematical modeling has emerged as an essential tool for guiding public health strategies, especially in low-income countries. Numerous models have been developed to analyze different aspects of dengue transmission, such as the impact of climate [2, 3], multi-serotype dynamics [4, 5], and human mobility [6, 7]. These approaches have helped identify key drivers of disease spread and assess potential control strategies.

Recent studies have also demonstrated the versatility of mathematical approaches in other contexts, such as online game addiction [8], competitive transmission of the omicron and delta COVID-19 variants [9], and mutated COVID-19 with imperfect vaccination [10]. These applications highlight the relevance of innovative modeling frameworks for understanding complex epidemiological dynamics like dengue transmission in Burkina Faso.

Our study is motivated by the 2023 dengue epidemic in Burkina Faso. Analysis of local data revealed a clear predominance of the DEN-3 serotype (81.8%), supporting a single–serotype approach. Building on the work of Zou et al. [11], we propose a model combining a susceptible–infected (SI) structure for the mosquito aquatic phase, a susceptible–exposed–infected (SEI) structure for adult mosquitoes, and a susceptible–exposed–infected–recovered (SEIR) framework for humans. The model incorporates two key features: vertical transmission in mosquitoes and the distinction between clinically detected and undetected human cases.

In the literature, dengue modeling studies in Burkina Faso remain limited. Few combine local data with metaheuristic algorithms for parameter estimation, and most overlook important biological features such as vertical transmission and partial clinical detection. To fill this gap, the present study applies, for the first time, the African vulture optimization algorithm (AVOA) to estimate model parameters from local data, providing a more accurate representation of dengue dynamics in the country.

Parameter estimation, which is challenging due to the model's strong nonlinearity, is formulated as an optimization problem solved using AVOA, a robust metaheuristic capable of identifying global solutions. This methodological innovation allows precise model calibration and effective simulation of dengue control strategies.

The paper is organized as follows: Section 2 presents the model formulation; Sections 3 and 4 provide the mathematical analysis and equilibrium stability; Section 5 describes the parameter estimation approach using AVOA; Section 6 presents the results and sensitivity analysis; Section 7 evaluates the control strategies through simulations; and Section 8 concludes with a summary and perspectives.

2. Model formulation

2.1. Model structure and compartment description

The model divides the total mosquito and human populations into several mutually exclusive compartments on the basis of on their epidemiological status.

- The **aquatic stage mosquito population**, $N_A(t)$, is divided into susceptibles, $S_A(t)$, and infected (through vertical transmission), $I_A(t)$. Thus, $N_A(t) = S_A(t) + I_A(t)$.
- The **adult female mosquito population**, $N_V(t)$, is stratified into susceptibles, $S_V(t)$, exposed (infected but not yet infectious), $E_V(t)$, and infectious, $I_V(t)$. Thus, $N_V(t) = S_V(t) + E_V(t) + I_V(t)$.
- The **human population**, $N_h(t)$, is subdivided into susceptibles, $S_h(t)$, exposed, $E_h(t)$, undetected infectious, $I_u(t)$, detected infectious, $I_d(t)$, and recovered, $R_h(t)$. Thus, $N_h(t) = S_h(t) + E_h(t) + I_u(t) + I_d(t) + R_h(t)$.

A detailed description of each variable is provided in Table 1.

Table 1. Description of the variables used in the model.

Variables	Biological description
$S_A(t)$	Susceptible aquatic mosquitoes
$I_A(t)$	Infected aquatic mosquitoes
$S_V(t)$	Susceptible adult mosquitoes
$E_V(t)$	Exposed adult mosquitoes
$I_V(t)$	Infectious adult mosquitoes
$S_h(t)$	Susceptible human population
$E_h(t)$	Exposed human population
$I_u(t)$	Undetected infectious human population
$I_d(t)$	Detected infectious human population
$R_h(t)$	Recovered human population

2.2. Assumptions and transmission mechanisms

The model is based on the following assumptions and mechanisms.

- **H1:** Only one serotype is considered.
- **H2: Human population:** The human population is considered open, with a constant birth rate (λ) and a natural death rate (μ). All new births enter the susceptible compartment (S_h).
- **H3: Mosquito population:** The mosquito population dynamics are regulated by a carrying capacity (k_A) at aquatic breeding sites. Egg laying follows a logistic growth function.
- **H4: Mortality:** Natural mortality is assumed to be constant for each population (human, aquatic, and adult). Additionally, dengue can induce extra mortality in infected humans, with distinct rates for detected cases (μ_d) and undetected cases (μ_u).
- **H5: Transmission cycle:** Dengue virus transmission follows a heterogeneous cycle: A mosquito becomes infected by biting an infectious human, and a human becomes infected by being bitten by an infectious mosquito. No direct human-to-human or mosquito-to-mosquito transmission is considered, except for vertical transmission.

- **H6: Force of infection:** The transmission law follows the **standard mass action** principle. The rate of new infections is proportional to the number of susceptible individuals and the prevalence of infectious individuals in the other population (human or vector).

$$\text{Force of infection on mosquitoes: } \lambda_m = b\beta_{mh}\frac{I_u + I_d}{N_h}.$$

$$\text{Force of infection on humans: } \lambda_h = b\beta_{hm}\frac{I_V}{N_h}.$$

- **H7: Vertical transmission:** A constant proportion (α_V) of eggs laid by infectious female mosquitoes is already infected. This mechanism is the only mosquito-to-mosquito transmission route.

Table 2. Parameters used in the model.

Parameters	Description
μ_A	Natural mortality rate of aquatic mosquitoes
k_A	Carrying capacity
μ_V	Natural mortality rate of adult mosquitoes
r_L	Larval development rate of aquatic mosquitoes
r_A	Maturation rate of aquatic mosquitoes into adults
α_V	Vertical transmission rate
β_{mh}	Probability that a susceptible mosquito gets infected after biting an infected human
β_{hm}	Probability that a susceptible human gets infected after being bitten by an infected mosquito
b	Mosquito biting rate
λ	Human birth rate
μ	Natural mortality rate of humans
μ_u	Disease-induced mortality rate of undetected infected humans
μ_d	Disease-induced mortality rate of detected infected humans
σ_V	Virus development rate
δ	Progression rate of humans from the exposed state to the infectious state
β	Proportion of detected infected humans
γ_u	Recovery rate of undetected infected humans
γ_d	Recovery rate of detected infected human

- **H8: Latency periods:** Newly infected humans and mosquitoes pass through a latency period (compartments E_h and E_V, respectively), during which they are infected but not yet infectious. The residence time in these compartments is assumed to be exponentially distributed, implying constant exit rates (δ and σ_V).

- **H9: Under-reporting of cases:** A constant proportion (β) of humans becoming infectious are detected by the health system (I_d), while the complementary proportion ($1-\beta$) is not reported (I_u). We assume that both groups are equally infectious to mosquitoes.
- **H10: Immunity:** Humans who recover from the disease (compartment R_h) are assumed to acquire permanent immunity and cannot be reinfected by the serotype considered in this study.
- **H11: Homogeneity:** Mixing within each population (human and vector) is assumed to be homogeneous. Every individual has the same probability of contacting any other individual in the other population.

The parameters are presented in Table 2, and the flows between compartments are schematically illustrated in Figure 1.

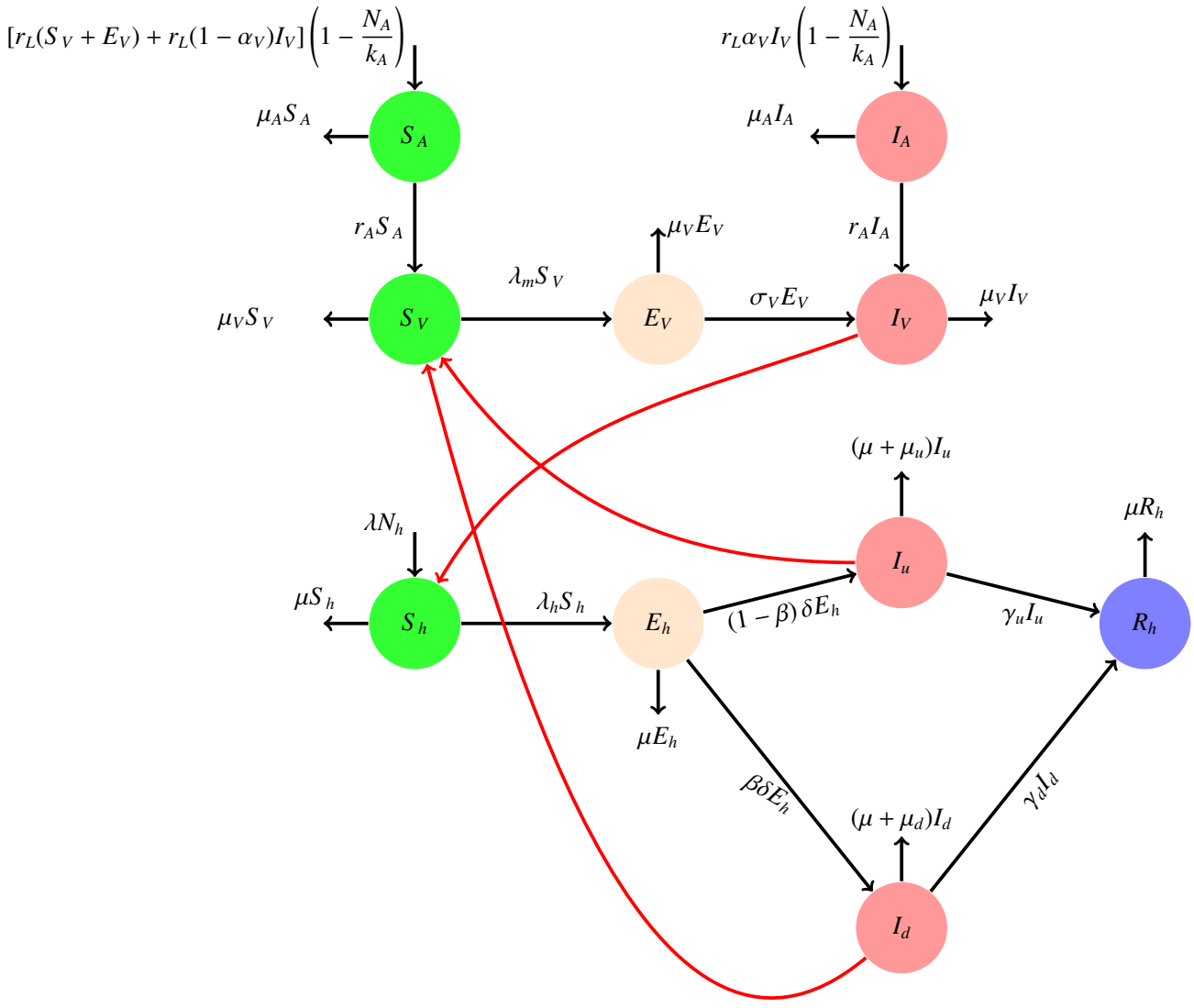

Figure 1. Diagram of the model of the transmission of dengue.

3. Mathematical analysis of our dengue model

3.1. Mathematical model

By performing a mass balance across the different compartments considered, we obtain the following system:

$$\begin{cases} \frac{dS_A}{dt} = \left[r_L\left(S_V + E_V\right) + r_L\left(1-\alpha_V\right)I_V\right]\left(1-\frac{N_A}{k_A}\right) - \left(\mu_A + r_A\right)S_A \\ \frac{dI_A}{dt} = r_L\alpha_V I_V\left(1-\frac{N_A}{k_A}\right) - \left(\mu_A + r_A\right)I_A \\ \frac{dS_V}{dt} = r_A S_A - b\beta_{mh}\left(\frac{I_d+I_u}{N_h}\right)S_V - \mu_V S_V \\ \frac{dE_V}{dt} = b\beta_{mh}\left(\frac{I_u+I_d}{N_h}\right)S_V - \mu_V E_V - \sigma_V E_V \\ \frac{dI_V}{dt} = \sigma_V E_V + r_A I_A - \mu_V I_V \\ \frac{dS_h}{dt} = \lambda N_h - \mu S_h - b\beta_{hm}\frac{I_V}{N_h}S_h. \\ \frac{dE_h}{dt} = b\beta_{hm}\frac{I_V}{N_h}S_h - \mu E_h - \delta E_h \\ \frac{dI_u}{dt} = (1-\beta)\delta E_h - \left(\mu + \mu_u + \gamma_u\right)I_u \\ \frac{dI_d}{dt} = \beta\delta E_h - (\mu + \mu_d)I_d - \gamma_d I_d \\ \frac{dR_h}{dt} = \gamma_u I_u + \gamma_d I_d - \mu R_h \\ S_A(0) = S_{A,0}, I_A(0) = I_{A,0}, S_V(0) = S_{V,0}, E_V(0) = E_{V,0}, I_V(0) = I_{V,0}, S_h(0) = S_{h,0} \\ E_h(0) = E_{h,0}, I_u(0) = I_{u,0}, I_d(0) = I_{d,0}, R_h(0) = R_{h,0}. \end{cases} \tag{3.1}$$

All 18 parameters: (μ_A, μ, r_L, r_A, σ_V, β_{hm}, β_{mh}, a, λ, μ_d, μ, μ_u, γ_u, γ_d, δ, and β) used for the dengue model are non-negative, since the models describes the dynamics of the human and mosquito populations.

3.2. Existence, uniqueness, positivity and boundedness of solutions

3.2.1. Existence and uniqueness of solutions

Theorem 3.1. *[12] Suppose that the functions appearing on the right-hand sides of the equations of System* (3.1) *and their partial derivatives with respect to* $S_A, I_A, S_V, E_V, I_V, S_h, E_h, I_u, I_d$, *and* R_h *are continuous in a rectangular domain according to* $a < t < b$, $c < S_A, I_A, S_V, E_V, I_V, S_h, E_h, I_u, I_d, R_h < d$. *Then for all* $t \in (a, b)$ *and* $S_{A,0}, I_{A,0}, S_{V,0}, E_{V,0}, I_{V,0}, S_{h,0}, E_{h,0}, I_{u,0}, I_{d,0}$, *and* $R_{h,0} \in (c, d)$, *the initial value problem of System* (3.1) *has a unique solution on an open interval* $a < \omega < t < \varphi < b$ *containing* t_0.

Proof. Let $x(t) = \left(S_A(t),\ I_A(t),\ S_V(t),\ E_V(t), I_V(t),\ S_h(t),\ E_h(t),\ I_d(t),\ I_u(t),\ R_h(t)\right)$,
$t \in (a, b)$ and $S_A(t),\ I_A(t),\ S_V(t),\ E_V(t),\ I_V(t),\ S_h(t),\ E_h(t),\ I_u(t),\ I_d(t),\ R_h(t) \in (c, d)$.
Then $x'(t) = \left(S_{A,0},\ I_{A,0},\ S_{V,0},\ E_{V,0},\ I_{V,0},\ S_{h,0},\ E_{h,0},\ I_{u,0},\ I_{d,0},\ R_{h,0}\right)$.

Let us define a function g such that:

$$g(x(t)) = \left(\frac{dS_A}{dt}, \frac{dI_A}{dt}, \frac{dS_V}{dt}, \frac{dE_V}{dt}, \frac{dI_V}{dt}, \frac{dS_h}{dt}, \frac{dE_h}{dt}, \frac{dI_u}{dt}, \frac{dI_d}{dt}, \frac{dR_h}{dt}\right).$$

Let $t_0 \in (a, b)$ and

$$x(t_0) = \Big(S_A(t_0),\, I_A(t_0),\, S_V(t_0),\, E_V(t_0), I_V(t_0),\, S_h(t_0),\, E_h(t_0),\, I_u(t_0),\, I_d(t_0),\, R_h(t_0)\Big)$$
$$= \Big(S_{A,0},\, I_{A,0},\, S_{V,0},\, E_{V,0},\, I_{V,0},\, S_{h,0},\, E_{h,0},\, I_{u,0},\, I_{d,0},\, R_{h,0}\Big) = x_0 \in (c, d).$$

By our hypothesis, we know that $g(x(t))$ and its partial derivative $g_x(x(t))$ are continuous in the rectangular domain $a < t < b$, $c < x < d$. The initial value problem:

$$\begin{cases} x'(t) = g(x(t)) \\ x(t_0) = x_0, \end{cases}$$

admits a unique solution valid on an open interval containing t_0.

3.2.2. Positivity of solutions

Theorem 3.2. *Let us consider the initial conditions $S_A(0) > 0$, $I_A(0) > 0$, $S_V(0) > 0$, $E_V(0) > 0$, $I_V(0) > 0$, $S_h(0) > 0$, $E_h(0) > 0$, $I_u(0) > 0$, $I_d(0) > 0$, and $R_h(0) > 0$. Then the solutions $S_A(t)$, $I_A(t)$, $S_V(t)$, $E_V(t)$, $I_V(t)$, $S_h(t)$, $E_h(t)$, $I_u(t)(t)$, $I_d(t)$, and $R_h(t)$ of System* (3.1) *are all positive for all $t > 0$.*

Proof. Suppose that $S_A(0) > 0$, $I_A(0) > 0$, $S_V(0) > 0$, $E_V(0) > 0$, $I_V(0) > 0$, $S_h(0) > 0$, $E_h(0) > 0$, $I_u(0) > 0$, $I_d(0) > 0$, and $R_h(0) > 0$. For all $t > 0$, we show that $S_A(t) > 0$, $I_A(t) > 0$, $S_V(t) > 0$, $E_V(t) > 0$, $I_V(t) > 0$, $S_h(t) > 0$, $E_h(t) > 0$, $I_u(0) > 0$, $I_d(0) > 0$, and $R_h(t) > 0$.

$$\frac{dS_A}{dt} = \Big[r_L\,(S_V + E_V) + r_L(T)\,(1 - \alpha_V)\,I_V\Big]\left(1 - \frac{N_A}{K_A}\right) - (\mu_A + r_A)\,S_A \tag{3.2}$$

$$\frac{dS_A}{S_A} \geq -\,[\mu_A + r_A]\,dt \tag{3.3}$$

This implies that:

$$S_A(t) \geq S_A(0)\exp\{-\int_0^t [\mu_A + r_A]\,dt\} > 0.$$

We also have:

$$\frac{dI_A}{dt} = r_L\alpha_V I_V\left(1 - \frac{N_A}{K_A}\right) - (\mu_A + r_A)\,I_A, \tag{3.4}$$

where

$$I_A(t) \geq I_A(0)\exp\{-\int_0^t [\mu_A + r_A]\,dt\} > O.$$

Using a similar approach, let us establish that:

$$S_V(t) \geq S_V(0)\exp\{-\int_0^t \left[b\beta_{mh}\left(\frac{I_u + I_d}{N_h}\right) + \mu_V\right] dt\} > O,$$
$$E_V(t) \geq E_V(0)\exp\{-\int_0^t (\mu_V + \sigma_V)\,dt\} > O,$$

$$I_V(t) \geq I_V(0)\exp\{-\int_0^t \mu_V dt\} > O,$$
$$S_h(t) \geq S_h(0)\exp\{-\int_0^t \left(b\beta_{hm}\frac{I_V}{N_h} + \mu\right) dt\} > O,$$
$$E_h(t) \geq E_h(0)\exp\{-\int_0^t (\delta + \mu)\, dt\} > O,$$
$$I_u(t) \geq I_u(0)\exp\{-\int_0^t (\gamma_N + \mu + \mu_u)\, dt\} > O,$$
$$I_d(t) \geq I_d(0)\exp\{-\int_0^t (\gamma_d + \mu + \mu_d)\, dt\} > O,$$
$$R_h(t) \geq R_h(0)\exp\{-\int_0^t \mu dt\} > O.$$

Thus, we have shown that all state variables of the model remain positive for all $t \geq 0$, which completes the proof. Therefore $N_h(t) \geq 0$, $N_A(t) \geq 0$, and $N_V(t) \geq 0$ are non-negative.

3.3. Boundedness of solutions

Proposition 3.3. *For System* (3.1)*, the solutions are bounded in the region.*

$$\Omega = \{(S_A, I_A, S_V, E_V, I_V, S_h, E_h, I_u, I_d, R_h)) \in \mathbb{R}^{10}_+ / N_A \leq k_A, N_V \leq \frac{r_A k_A}{\mu_V}, N_h \leq \frac{k_1}{\mu}\}, \tag{3.5}$$

with $N_A = S_A + I_A$, $N_V = S_V + E_V + I_V$ *and* $N_h = S_h + E_h + I_u + I_d + R_h$.

We observe that

- $\frac{dN_A}{dt} = r_L N_V\left(1 - \frac{N_A}{k_A}\right) - (\mu_A + r_A)N_A$,
  $N_A \leq k_A$;
- $\frac{dN_V}{dt} = r_A N_A - \mu_V N_V$,
  $N_V(t) \leq N_{V,0}e^{-\mu_V t} + \frac{r_A N_A}{\mu_V}$;
- $\frac{dN_H(t)}{dt} = k_1 - \mu N_H(t) - \mu_u I_u - \mu_d I_d$ with $k_1 = \lambda N_h$ = recruitment rate,
  $N_h(t) \leq N_{h,0}e^{-\mu t} + \frac{k_1}{\mu}$.

Since $t \to +\infty$, we have $0 \leq (N_A(t), N_V(t), N_(t)) \leq \left(k_A, \frac{r_A N_A}{\mu_V}, \frac{k_1}{\mu}\right)$. Hence, the solutions of System (3.1) are bounded in Ω.

3.4. Reproduction number and disease free-equilibrium

3.4.1. The net reproductive number

From System (3.1), we define the following system for populations of aquatic mosquitoes, adult mosquitoes, and humans:

$$\begin{cases} \frac{dN_A}{dt} = r_L N_V \left(1 - \frac{N_A}{k_A}\right) - (r_A + \mu_A) N_A \\ \frac{dN_V}{dt} = r_A N_A - \mu_V N_V \\ \frac{dN_h}{dt} = k_1 - \mu N_H - \mu_u I_u - \mu_d I_d. \end{cases} \tag{3.6}$$

The net reproductive number of the System (3.6) is defined as follows:

$$r_0 = \frac{r_A r_L}{\mu_V (r_A + \mu_A)}. \tag{3.7}$$

We have the following theorem.

Theorem 3.4. *Model* (3.1) *has two disease-free equilibria depending on the magnitude of* r_0.

- *If* $r_0 < 1$*, then there is a trivial equilibrium point (without mosquitoes and without disease), or TDFE (trivial disease-free equilibrium) denoted* $\mathcal{E}_0^*$ *and defined by*
  $\mathcal{E}_0^* = (S_A^*, I_A^*, S_V^*, E_V^*, I_V^*, S_h^*, E_h^*, I_u^*, I_d^*, R_h^*)$*;*
  $\mathcal{E}_0^* = (0, 0, 0, 0, 0, \frac{k_1}{\mu}, 0, 0, 0, 0)$.

- *Si* $r_0 > 1$*, then there is a non-trivial equilibrium point (without disease but with the presence of mosquitoes), NDFE (non-trivial disease-free equilibrium) denoted* $\mathcal{E}_0^{**}$ *and defined by*
  $\mathcal{E}_0^{**} = (S_A^{**}, I_A^{**}, S_V^{**}, E_V^{**}, I_V^{**}, S_h^{**}, E_h^{**}, I_u^{**}, I_d^{**}, R_h^{**})$*;*
  $\mathcal{E}_0^{**} = \left(k_A\left(1 - \frac{1}{r_0}\right), 0, \frac{r_A k_A}{\mu_V}\left(1 - \frac{1}{r_0}\right), 0, 0, \frac{k_1}{\mu}, 0, 0, 0, 0\right)$.

To determine the disease-free equilibrium points of the model, we assume that there is no variation over time in the state variables.

In the absence of disease, the rate of infection by vertical transmission is zero in the human and mosquito populations. So we have $\alpha_V = 0$, and $I_A = 0$. To determine the equilibrium points, we cancel

certain equations of System (3.1), we have:

$$\begin{cases} [r_L(S_V + E_V) + r_L(1-\alpha_V)I_V]\left(1 - \dfrac{N_A}{k_A}\right) - (\mu_A + r_A)S_A = 0 \\ r_L\alpha_V I_V\left(1 - \dfrac{N_A}{k_A}\right) - (\mu_A + r_A)I_A = 0 \\ r_A S_A - \lambda_m S_V - \mu_V S_V = 0 \\ \lambda_m S_V - \mu_V(T)E_V - \sigma_V E_V = 0 \\ \sigma_V E_V + r_A I_A - \mu_V I_V = 0 \\ k_1 - \mu S_h - \lambda_h S_h = 0 \\ \lambda_h S_h - \mu E_h - \delta E_h = 0 \\ (1-\beta)\delta E_h - (\mu + \mu_u + \gamma_u)I_u = 0 \\ \beta\delta E_h - (\mu + \mu_d + \gamma_d)I_d = 0 \\ \gamma_u I_u + \gamma_d I_d - \mu R_h = 0. \end{cases} \tag{3.8}$$

Solving the equations for the humans in System (3.8), we obtain:

$$S_h = \frac{k_1}{\lambda_h + \mu},$$

$$E_h = \frac{\lambda_h k_1}{(\delta + \mu)(\lambda_h + \mu)},$$

$$I_u = \frac{(1-\beta)\delta\lambda_h k_1}{(\mu + \mu_u + \gamma_u)(\delta + \mu)(\lambda_h + \mu)},$$

$$I_d = \frac{\beta\delta\lambda_h k_1}{(\mu + \mu_d + \gamma_d)(\delta + \mu)(\lambda_h + \mu)},$$

$$R_h = \frac{\delta\lambda_h k_1}{\mu(\mu + \lambda_h)(\mu + \delta)}\left(\frac{\gamma_u(1-\beta)}{\mu + \mu_u + \gamma_u} + \frac{\gamma_d\beta}{\mu + \mu_d + \gamma_d}\right).$$

Let us solve the equations for adult mosquitoes at the disease-free equilibrium points. We have:

$$S_V = \frac{r_A S_A}{\lambda_m + \mu_V},$$

$$E_V = \frac{r_A\lambda_m S_A}{(\sigma_V + \mu_V)(\lambda_M + \mu_V)},$$

$$I_V = \frac{\sigma_V r_A\lambda_m S_A}{\mu_V(\sigma_V + \mu_V)(\lambda_m + \mu_V)}.$$

- Trivial disease-free equilibrium (mosquito-free) (TDFE)
  $S_A = 0$, $I_A = 0$, $S_V = 0$, $E_V = 0$, $I_V = 0$,$S_h = \dfrac{k_1}{\mu}$, $E_h = 0$, I_u, $I_d = 0$, $R_h = 0$.
  $\mathcal{E}_0^* = (0, 0, 0, 0, 0, \dfrac{k_1}{\mu}, 0, 0, 0, 0)$.
- Non trivial disease-free equilibrium (with the presence of mosquitoes) (NDFE)
  $N_V = S_V + E_V + I_V$, Therefore, with
  $N_V = \dfrac{r_L r_A}{\mu_V}$ in the first equation of System (3.8), let us substitute N_V with its expression and solve:
  $S_A\left(\dfrac{r_L r_A}{\mu_V} - (\mu_A + r_A) - \dfrac{S_A r_L r_A}{\mu_V k_A}\right) = 0$ and thus

$S_A^{**} = k_A\left(1 - \frac{1}{r_0}\right)$.

From the third equation, we have: $S_V = \frac{r_A S_A}{\mu_V} = \frac{r_A k_A}{\mu_V}\left(1 - \frac{1}{r_0}\right)$,

$\mathcal{E}_0^{**} = \left(k_A\left(1 - \frac{1}{r_0}\right), 0, \frac{r_A k_A}{\mu_V}\left(1 - \frac{1}{r_0}\right), 0, 0, \frac{k_1}{\mu}, 0, 0, 0, 0\right)$.

3.4.2. Basic reproduction number

To determine the expression of the basic reproduction number, we use the next-generation matrix method described by P. van den Driessche and J. Watmough in [13].

From System (3.1), we define $\frac{dX}{dt} = \mathcal{F}(X) - \mathcal{V}(X)$, where $X = (E_h, I_u, I_d, E_V, I_V, I_A, S_h, R_h, S_V, S_A)$.

Here, $\mathcal{F}(X)$ represents the rate of appearance of new infections in each compartment, and $\mathcal{V}(X) = \mathcal{V}^-(X) - \mathcal{V}^+(X)$, where:

- $\mathcal{V}^+(X)$ is the rate of entry of individuals into the infected compartments due to means other than new infections (e.g., progression or transition);
- $\mathcal{V}^-(X)$ is the rate of removal from the infected compartments (e.g., recovery, death).

Consequently, we construct the matrices $\mathcal{F}$ and $\mathcal{V}$ by identifying the new infection terms and the transfer terms, respectively, within the infected compartments. These will be used to determine the next-generation matrix and compute the basic reproduction number $\mathcal{R}_0$.

$$\mathcal{F} = \begin{pmatrix} b\beta_{hm}\frac{I_V}{N_h}S_h \\ 0 \\ 0 \\ b\beta_{mh}\left(\frac{I_d+I_u}{N_h}\right)S_V \\ 0 \\ r_L\alpha_V I_V\left(1 - \frac{N_A}{K_A}\right) \\ 0 \\ 0 \\ 0 \\ 0 \end{pmatrix}.$$

$$\mathcal{V} = \begin{pmatrix} (\mu+\delta)E_h \\ (\mu+\mu_u+\gamma_u)I_u - (1-\beta)\delta E_h \\ (\mu+\mu_d+\gamma_d)I_d - \beta\delta E_h \\ (\mu_V+\sigma_V)E_V \\ \mu_V I_V - \sigma_V E_V - r_A I_A \\ (\mu_A+r_A)I_A \\ b\beta_{mh}\frac{I_V}{N_h}S_h + \mu S_h - k_1 \\ \mu R_h - \gamma_u I_u - \gamma_d I_d \\ b\beta_{mh}\left(\frac{I_d+I_u}{N_h}\right)S_V + \mu_V S_V - r_A S_A \\ (\mu_A+r_A)S_A - [r_L(S_V+E_V) + r_L(1-\alpha_V)I_V]\left(1 - \frac{N_A}{k_A}\right) \end{pmatrix}.$$

The Jacobian matrices of $\mathcal{F}(X)$ and $\mathcal{V}(X)$ at the point $\mathcal{E}_0^{**}$ are, respectively

$$D\mathcal{F}_{x_0} = \begin{pmatrix} F & 0 \\ 0 & 0 \end{pmatrix}, \quad D\mathcal{V}_{x_0} = \begin{pmatrix} V & 0 \\ J_3 & J_4 \end{pmatrix},$$

$$V = \begin{pmatrix} j_4 & 0 & 0 & 0 & 0 & 0 \\ j_5 & j_6 & 0 & 0 & 0 & 0 \\ j_7 & 0 & j_8 & 0 & 0 & 0 \\ 0 & 0 & 0 & j_9 & 0 & 0 \\ 0 & 0 & 0 & -\sigma_V & \mu_V & -r_A \\ 0 & 0 & 0 & 0 & 0 & j_{10} \end{pmatrix},$$

$$F = \begin{pmatrix} 0 & 0 & 0 & 0 & j_1 & 0 \\ 0 & 0 & 0 & 0 & 0 & 0 \\ 0 & 0 & 0 & 0 & 0 & 0 \\ 0 & j_2 & j_2 & 0 & 0 & 0 \\ 0 & 0 & 0 & 0 & 0 & 0 \\ 0 & 0 & 0 & 0 & j_3 & 0 \end{pmatrix},$$

$$j_1 = b\beta_{hm}, \quad j_2 = \frac{b\beta_{mh}\mu k_A}{\mu_v r_L k_1}\left(r_A r_L - \mu_v(r_A + \mu_A)\right),$$

$$j_3 = \frac{\alpha_v \mu_v (r_A + \mu_A)}{r_A}, \quad j_4 = \mu + \delta, \quad j_5 = -(1-\beta)\delta,$$

$$j_6 = \mu + \mu_u + \gamma_u, \quad j_7 = -\beta\delta, \quad j_8 = \mu + \mu_d + \gamma_d,$$

$$j_9 = \mu_v + \sigma_v, \quad j_{10} = \mu_A + r_A.$$

$$V^{-1} = \begin{pmatrix} \frac{1}{j_4} & 0 & 0 & 0 & 0 & 0 \\ -\frac{j_5}{j_4 j_6} & \frac{1}{j_6} & 0 & 0 & 0 & 0 \\ \frac{j_5 j_7}{j_4 j_6 j_8} - \frac{j_7}{j_4 j_8} & 0 & \frac{1}{j_8} & 0 & 0 & 0 \\ 0 & 0 & 0 & \frac{1}{j_9} & 0 & 0 \\ 0 & 0 & 0 & \frac{\sigma_v}{j_9 \mu_v} & \frac{1}{\mu_v} & \frac{r_A}{\mu_v j_{10}} \\ 0 & 0 & 0 & 0 & 0 & \frac{1}{j_{10}} \end{pmatrix},$$

$$FV^{-1} = \begin{pmatrix} 0 & 0 & 0 & P_{54}j_1 & P_{55}j_1 & P_{56}j_1 \\ 0 & 0 & 0 & 0 & 0 & 0 \\ 0 & 0 & 0 & 0 & 0 & 0 \\ P_{21}j_2 + P_{31}j_2 & P_{22}j_2 & P_{33}j_2 & 0 & 0 & 0 \\ 0 & 0 & 0 & 0 & 0 & 0 \\ 0 & 0 & 0 & P_{54}j_3 & P_{55}j_3 & P_{56}j_3 \end{pmatrix},$$

$$\lambda_1 = 0,$$

$$\lambda_2 = 0,$$
$$\lambda_3 = 0,$$
$$\lambda_4 = 0,$$
$$\lambda_5 = \frac{P_{56}j_3}{2} - \frac{1}{2}\sqrt{P_{56}^2 j_3^2 + 4(P_{21}+P_{31})P_{54}j_1 j_2},$$
$$\lambda_6 = \frac{P_{56}j_3}{2} + \frac{1}{2}\sqrt{P_{56}^2 j_3^2 + 4(P_{21}+P_{31})P_{54}j_1 j_2}.$$

The basic reproduction number associated with the model is given by the spectral radius of the next-generation matrix, that is, its dominant eigenvalue. It follows that:

$$\mathcal{R}_0 = \frac{P_{56}j_3}{2} + \frac{1}{2}\sqrt{P_{56}^2 j_3^2 + 4(P_{21}+P_{31})P_{54}j_1 j_2},$$

$$P_{11} = \frac{1}{j_4}, \quad P_{21} = -\frac{j_5}{j_4 j_6}, \quad P_{22} = \frac{1}{j_6}, \quad P_{31} = -\frac{j_7}{j_4 j_8},$$
$$P_{33} = \frac{1}{j_8}, \quad P_{44} = \frac{1}{j_9}, \quad P_{54} = \frac{\sigma_V}{\mu v j_9}, \quad P_{55} = \frac{1}{\mu_V}, \quad P_{56} = \frac{r_A}{\mu_V j_{10}}, \quad P_{66} = \frac{1}{j_{10}},$$

$$\mathcal{R}_0 = \frac{\alpha_v}{2} + \frac{1}{2}\sqrt{\alpha_v^2 + 4D},$$

$$D = \left[\frac{\delta}{\mu+\delta}\left(\frac{1-\beta}{\mu+\mu_u+\gamma_u} + \frac{\beta}{\mu+\mu_d+\gamma_d}\right)\right]\cdot\left[\frac{b^2\beta_{hm}\beta_{mh}\mu k_A\sigma_v}{\mu_v^2(\mu_v+\sigma_v)r_L k_1}\cdot(r_A r_L - \mu_v(r_A+\mu_A))\right].$$

3.5. Global stability of the equilibrium point

3.5.1. Global stability of the trivial equilibrium point

Theorem 3.5. *If $r_0 < 1$, then the TDFE is globally asymptotically stable.*

Proof. To prove the theorem, we use the approach used in [14]. When $r_0 \leq 1$, there is a unique equilibrium point without disease. Let's rewrite the System (3.1) in the following matrix for M:

$$\frac{dX}{dt} = A(X)X + U, \tag{3.9}$$

where $X = (S_A, I_A, S_V, E_V, I_V, S_h, E_h, I_u, I_d, R_h,)^T$; $U = (0,0,0,0,0,k_1,0,0,0,0,0)^T$ and $A(X)$ is a 10×10 matrix defined by

$$A(X) = \begin{pmatrix} b_{11} & 0 & b_{13} & b_{14} & b_{15} & 0 & 0 & 0 & 0 & 0 \\ 0 & b_{22} & 0 & 0 & b_{25} & 0 & 0 & 0 & 0 & 0 \\ r_A & 0 & b_{33} & 0 & 0 & 0 & 0 & 0 & 0 & 0 \\ 0 & 0 & b_{43} & b_{44} & 0 & 0 & 0 & 0 & 0 & 0 \\ 0 & r_A & 0 & \sigma_V & -\mu_V & 0 & 0 & 0 & 0 & 0 \\ 0 & 0 & 0 & 0 & 0 & b_{66} & 0 & 0 & 0 & 0 \\ 0 & 0 & 0 & 0 & 0 & b_{76} & b_{77} & 0 & 0 & 0 \\ 0 & 0 & 0 & 0 & 0 & 0 & (1-\beta)\delta & b_{88} & 0 & 0 \\ 0 & 0 & 0 & 0 & 0 & 0 & \beta\delta & 0 & b_{99} & 0 \\ 0 & 0 & 0 & 0 & 0 & 0 & 0 & \gamma_u & \gamma_d & -\mu \end{pmatrix}, \tag{3.10}$$

with:
$b_{11} = -(r_A + \mu_A)$, $b_{13} = b_{14} = r_L\left(1 - \frac{N_A}{K_A}\right)$, $b_{15} = r_L(1-\alpha_V)\left(1 - \frac{N_A}{K_A}\right)$, $b_{22} = -(r_A + \mu_A)$,
$b_{25} = r_L\alpha_V\left(1 - \frac{N_A}{K_A}\right)$, $b_{33} = -b\beta_{mh}\left(\frac{I_u+I_d}{N_h}\right) - \mu_V$, $b_{43} = b\beta_{mh}\frac{I_u+I_d}{N_h}$, $b_{44} = -(\sigma_V + \mu_V)$,
$b_{66} = -b\beta_{hm}\left(\frac{I_V}{N_h}\right) - \mu$, $b_{76} = b\beta_{hm}\left(\frac{I_V}{N_h}\right)$, $b_{77} = -(\delta + \mu)$, $b_{88} = -(\gamma_u + \mu + \mu_u)$, $b_{99} = -(\gamma_d + \mu)$.

Let $Y = X - TDFE$.

Thus, Eq (3.9) can be rewritten

$$\frac{dY}{dt} = A(Y)Y. \tag{3.11}$$

It is clear that $TDFE_Y = (0, 0, 0, 0, 0, 0, 0, 0, 0, 0)$ is the unique equilibrium point of System (3.11). Consider the Lyapunov function

$$V(Y) =< W, Y >,$$

with $W = (\frac{1}{r_L}, \frac{1}{r_L}, \frac{1}{\mu_V}, \frac{1}{\mu_V}, \frac{1}{\mu_V}, 1, 1, 1, 1, 1) > 0$.

We then have

$$\frac{dV}{dY} = \langle W, A(Y)Y\rangle.$$

We obtain:

$$\frac{dV}{dY} = \frac{r_A}{\mu_V}(1 - \frac{1}{r_0})(y_1 + y_2) - \frac{N_A}{k_A}(y_3 + y_4 + y_5) - \mu(y_7 + y_8 + y_9 + y_{10}) - \mu_N y_8.$$

Since $r_0 \leq 1$, it is obvious that $\frac{dV}{dY} \leq 0$. Furthermore, it follows from LaSalle's invariance principle that the maximal invariant set contained in $\left\{V|\frac{dV}{dY} = 0\right\}$ is the $TDFE_Y$. Thus, the transformed equilibrium $TDFE_Y$ is globally asymptotically stable if $r_0 \leq 1$. Therefore, $\mathcal{E}_0^*$ is also globally asymptotically stable if $r_0 \leq 1$.

3.6. Global stability of the non-trivial equilibrium point

In this section, we demonstrate the global asymptotic stability (GAS) of the NDFE point $\mathcal{E}_0^{**}$. To this end, we introduce the following theorem:

Theorem 3.6. *When* $\mathcal{R}_0 < 1$ *then* $\mathcal{E}_0^{**} = \left(k_A\left(1 - \frac{1}{r_0}\right), 0, \frac{r_A k_A}{\mu_V}\left(1 - \frac{1}{r_0}\right), 0, 0, \frac{k_1}{\mu}, 0, 0, 0, 0\right)$ *is GAS if* $\frac{S_V^{**}}{N_h^{**}} \geq \frac{S_V}{N_h}$, $N_A \geq N_A^{**}$ *et* $\frac{S_h^{**}}{N_h^{**}} \geq \frac{S_h}{N_h}$.

Proof. To prove this theorem, we adopt the Castillo-Chavez method [15].

We start by rewriting System (3.1) as follows:

$$\begin{cases} \frac{dX}{dt} = F(X, Y) \\ \frac{dY}{dt} = G(X, Y) \\ G(X, 0) = 0. \end{cases} \tag{3.12}$$

where $X = (S_A, S_V, S_h, R_h)^T$ designates the set of uninfected compartments and $Y = (I_A, E_V, I_V, E_h, I_u, I_d)^T$ designates all infected compartments.

$$F(X,Y) = \begin{pmatrix} [r_L(S_V + E_V) + r_L(1-\alpha_V)I_V]\left(1 - \frac{N_A}{K_A}\right) - (\mu_A + r_A)S_A \\ r_A S_A - b\beta_{mh}\left(\frac{I_d+I_u}{N_h}\right)S_V - \mu_V(T)S_V \\ k_1 - \mu S_h - b\beta_{hm}\frac{I_V}{N_h}S_h \\ \gamma_u I_u + \gamma_d I_d - \mu R_h \end{pmatrix}, \tag{3.13}$$

and

$$G(X,Y) = \begin{pmatrix} r_L\alpha_V I_V\left(1 - \frac{N_A}{K_A}\right) - (\mu_A + r_A)I_A \\ b\beta_{mh}\left(\frac{I_d+I_u}{N_h}\right)S_V - \mu_V E_V - \sigma_V E_V \\ \sigma_V E_V + r_A I_A - \mu_V I_V \\ b\beta_{hm}\frac{I_V}{N_h}S_h - \mu E_h - \delta E_h \\ (1-\beta)\delta E_h - (\mu + \mu_u + \gamma_u)I_u \\ \beta\delta E_h - \mu I_d - \gamma_d I_d \end{pmatrix}. \tag{3.14}$$

It is obvious that $G(X, 0) = 0$ at the disease-free equilibrium point. We now need to prove that (C_1) is satisfied. To this end, we calculate the eigenvalues of the Jacobian associated with $F(X, Y)$ in $\mathcal{E}_0^{**}$. Therefore,

$$\mathcal{J}_F(\mathcal{E}_0^{**}) = \begin{pmatrix} -(r_A + \mu_A) & r_L\left(1 - \frac{N_A^{**}}{k_A}\right) & 0 & 0 \\ r_A & -\mu_V & 0 & 0 \\ 0 & 0 & -\mu & 0 \\ 0 & 0 & 0 & -\mu \end{pmatrix}. \tag{3.15}$$

Its characteristic equation is: $\lambda(\mu + \lambda)^2(r_A + \mu_A + \mu_V + \lambda) = 0$. The eigenvalues of the matrix $\lambda_1 = 0$, $\lambda_2 = -\mu$, and $\lambda_3 = -(r_A + \mu_A + \mu_V)$ are zero or negative. Therefore, $\mathcal{E}_0^{**}$ is a globally and asymptotically stable equilibrium point. The next step is to validate the second condition: $G(X, Y) = BY - \overline{G}(X, Y)$, where $\overline{G}(X, Y) \geq 0$ for $(X, Y) \in \Delta$ we first calculate the matrix $B = \mathcal{J}_G(X, Y)$ at the disease-free equilibrium (DFE) point.

$$B = \begin{pmatrix} -r_A - \mu_A & 0 & r_L\alpha_V\left(1 - \frac{N_A^{**}}{k_A}\right) & 0 & 0 & 0 \\ 0 & -\sigma_V - \mu_V & 0 & 0 & b\beta_{mh}\frac{S_V^{**}}{N_h^{**}} & b\beta_{mh}\frac{S_V^{**}}{N_h^{**}} \\ r_A & \sigma_V & -\mu_V & 0 & 0 & 0 \\ 0 & 0 & b\beta_{hm}\frac{S_h^{**}}{N_h^{**}} & -\delta - \mu & 0 & 0 \\ 0 & 0 & 0 & (1-\beta)\delta & -\mu - \mu_u - \gamma_u & 0 \\ 0 & 0 & 0 & \beta\delta & 0 & -\mu - \gamma_d \end{pmatrix} \tag{3.16}$$

$$\bar{G}(X,Y)=\begin{pmatrix} -r_A-\mu_A & 0 & r_L\alpha_V\left(1-\frac{N_A^{**}}{k_A}\right) & 0 & 0 & 0 \\ 0 & -\sigma_V-\mu_V & 0 & 0 & b\beta_{mh}\frac{S_V^{**}}{N_h^{**}} & b\beta_{mh}\frac{S_V^{**}}{N_h^{**}} \\ r_A & \sigma_V & -\mu_V & 0 & 0 & 0 \\ 0 & 0 & b\beta_{hm}\frac{S_h^{**}}{N_h^{**}} & -\delta-\mu & 0 & 0 \\ 0 & 0 & 0 & (1-\beta)\delta & -\mu-\mu_u-\gamma_u & 0 \\ 0 & 0 & 0 & \beta\delta & 0 & -\mu-\gamma_d \end{pmatrix}\begin{pmatrix} I_A \\ E_V \\ I_V \\ E_h \\ I_u \\ I_d \end{pmatrix}-\begin{pmatrix} r_L\alpha_V I_V\left(1-\frac{N_A}{K_A}\right)-(\mu_A+r_A)\,I_A \\ b\beta_{mh}\left(\frac{I_d+I_u}{N_h}\right)S_V-\mu_V E_V-\sigma_V E_V \\ \sigma_V E_V+r_A I_A-\mu_V I_V \\ b\beta_{hm}\frac{I_V}{N_h}S_h-\mu E_h-\delta E_h \\ (1-\beta)\delta E_h-(\mu+\mu_u+\gamma_u)\,I_u \\ \beta\delta E_h-\mu I_d-\gamma_d I_d \end{pmatrix} \tag{3.17}$$

We obtain:

$$\bar{G}(X_1,X_2)=\begin{pmatrix} r_L\alpha_V I_V\left(\frac{N_A-N_A^{**}}{k_A}\right) \\ b\beta_{mh}(I_u+I_d)\left(\frac{S_V^{**}}{N_h^{**}}-\frac{S_V}{N_h}\right) \\ 0 \\ b\beta_{hm}I_V\left(\frac{S_h^{**}}{N_h^{**}}-\frac{S_h}{N_h}\right) \\ 0 \\ 0 \end{pmatrix}. \tag{3.18}$$

The matrix B is a Metzler matrix because its diagonal elements are all negative and its off-diagonal elements are all positive. Furthermore, $G(X,0)=(0,0,0,0,0,0)^T$. If $\frac{S_V^{**}}{N_h^{**}}\geq\frac{S_V}{N_h}$, $N_A\geq N_A^{**}$ and $\frac{S_h^{**}}{N_h^{**}}\geq\frac{S_h}{N_h}$ alors $\bar{G}(X,Y)\geq 0$. Therefore, both hypotheses are satisfied. On the basis of the Castillo-Chavez method [15–17], we demonstrate that if $\mathcal{R}_0<1$, the disease-free equilibrium point is globally asymptotically stable.

4. Endemic equilibrium point

This section analyzes the global stability of the model's endemic equilibrium. The proof is based on the use of Lyapunov functions. Global asymptotic stability means that; for any initial condition within a

neighborhood of the endemic equilibrium, the system's dynamics converge to this state over time.

4.1. Existence and local stability of the endemic equilibrium

Theorem 4.1. *System* (3.1) *admits a unique endemic equilibrium point denoted* $\mathcal{E}_0^{***}$ *of the components* $(N_A^{***}, I_A^{***}, N_V^{***}, E_V^{***}, I_V^{***}, N_h^{***}, S_h^{***}, E_h^{***}, I_u^{***}, I_d^{***})$ *which is locally asymptotically stable when* $R_0 > 1$ *and is unstable otherwise.*

Proof. To determine the endemic equilibrium, we analyze the positive solutions of the system below:

$$\begin{cases} r_L N_V \left(1 - \dfrac{N_A}{k_A}\right) - (r_A + \mu_A) N_A = 0 \\ r_L \alpha_V I_V \left(1 - \dfrac{N_A}{k_A}\right) - (r_A + \mu_A) I_A = 0 \\ r_A\, N_A - \mu_V N_V = 0 \\ b\beta_{mh} S_V \left(\dfrac{I_d + I_u}{N_h}\right) - (\sigma_V + \mu_V) E_V = 0 \\ r_A\, I_A + \sigma_V E_V - \mu_V I_V = 0 \\ k_1 - \mu N_h - \mu_u I_u - \mu_d I_d = 0 \\ k_1 - b\beta_{hm} S_h \dfrac{I_V}{N_h} - \mu S_h = 0 \\ b\beta_{hm} S_h \dfrac{I_V}{N_h} - \delta\, E_h - \mu\, E_h = 0 \\ (1-\beta)\,\delta E_h - (\mu + \mu_u + \gamma_u) I_u = 0 \\ \beta\delta E_h - (\mu + \mu_d + \gamma_d) I_d = 0. \end{cases} \tag{4.1}$$

Using the equations of System (4.1), we obtain:

$$N_A^{***} = \frac{k_A}{r_L\, r_A} \left[r_L\, r_A - \mu_V (r_A + \mu_A)\right],$$

$$N_V^{***} = \frac{k_A}{r_L \mu_V} \left[r_L\, r_A - \mu_V (r_A + \mu_A)\right],$$

$$I_A^{***} = \frac{\alpha_V \mu_V}{r_A} I_V^{***},$$

$$E_V^{***} = \frac{\mu_V\,(1 - \alpha_V)}{\sigma_V} I_V^{***},$$

$$N_h^{***} = \frac{k_1 - \mu_u\, I_u^{***} - \mu_d\, I_d^{***}}{\mu},$$

$$S_h^{***} = \frac{k_1 N_h^{***}}{b\beta_{hm} I_V^{***} + \mu N_h^{***}},$$

$$E_h^{***} = \frac{b\beta_{hm} k_1 I_V^{***}}{\left(b\beta_{hm} I_V^{***} + \mu N_h^{***}\right)(\delta + \mu)},$$

$$I_u^{***} = \frac{(1-\beta)\delta b\beta_{hm}k_1 I_V^{***}}{\left(b\beta_{hm}I_V^{***} + \mu N_h\right)(\delta+\mu)(\mu+\mu_u+\gamma_u)},$$

$$I_d^{***} = \frac{\beta\delta b\beta_{hm}k_1 I_V^{***}}{\left(b\beta_{hm}I_V^{***} + \mu N_h^{***}\right)(\delta+\mu)(\mu+\mu_d+\gamma_d)},$$

$$I_V^{***} = \frac{r_A I_A^{***} + \sigma_V E_V^{***}}{\mu_V}.$$

4.2. Global stability of the endemic equilibrium

In this section, using an appropriate Lyapunov function, we will show that the endemic equilibrium point is globally asymptotically stable, $\mathcal{E}^{***}$.

Theorem 4.2. *If $\mathcal{R}_0 > 1$, the endemic equilibrium point $\mathcal{E}^{***}$ of System* (3.1) *is globally asymptotically stable.*

Proof. Let V be the Lyapunov function defined by:

$$\begin{aligned}
V(X) &= (S_A - S_A^{***}) + (I_A - I_A^{***}) - (S_A^{***} + I_A^{***})\ln\left(\frac{S_A + I_A}{S_A^{***} + I_A^{***}}\right)\\
&\quad + (S_V - S_V^{***}) + (E_V - E_V^{***}) + (I_V - I_V^{***}) - (S_V^{***} + E_V^{***} + I_V^{***})\ln\left(\frac{S_V + E_V + I_V}{S_V^{***} + E_V^{***} + I_V^{***}}\right)\\
&\quad + (S_h - S_h^{***}) + (E_h - E_h^{***}) + (I_u - I_u^{***}) + (I_d - I_d^{***}) + (R_h - R_h^{***})\\
&\quad - (S_h^{***} + E_h^{***} + I_u^{***} + I_d^{***} + R_h^{***})\ln\left(\frac{S_h + E_h + I_u + I_d + R_h}{S_h^{***} + E_h^{***} + I_u^{***} + I_d^{***} + R_h^{***}}\right).
\end{aligned}$$

We have $V(X^{***}) = 0$.

$$\begin{aligned}
V(X(t)) &= (S_A + I_A) - (S_A^{***} + I_A^{***}) - (S_A^{***} + I_A^{***})\ln\left(\frac{S_A + I_A}{S_A^{***} + I_A^{***}}\right)\\
&\quad + (S_V + E_V + I_V) - (S_V^{***} + E_V^{***} + I_V^{***}) - (S_V^{***} + E_V^{***} + I_V^{***})\ln\left(\frac{S_V + E_V + I_V}{S_V^{***} + E_V^{***} + I_V^{***}}\right)\\
&\quad + (S_h + E_h + I_u + I_d + R_h) - (S_h^{***} + E_h^{***} + I_u^{***} + I_d^{***} + R_h^{***})\\
&\quad - (S_h^{***} + E_h^{***} + I_u^{***} + I_d^{***} + R_h^{***})\ln\left(\frac{S_h + E_h + I_u + I_d + R_h}{S_h^{***} + E_h^{***} + I_u^{***} + I_d^{***} + R_h^{***}}\right),
\end{aligned}$$

$$\begin{aligned}
V(X(t)) &= S_A - S_A^{***} - S_A^{***}\ln\frac{S_A}{S_A^{***}} + I_A - I_A^{***} - I_A^{***}\ln\frac{I_A}{I_A^{***}} + S_V - S_V^{***} - S_V^{***}\ln\frac{S_V}{S_V^{***}}\\
&\quad + E_V - E_V^{***} - E_V^{***}\ln\frac{E_V}{E_V^{***}} I_V - I_V^{***} - I_V^{***}\ln\frac{I_V}{I_V^{***}} + S_h - S_h^{***} - S_h^{***}\ln\frac{S_h}{S_h^{***}}\\
&\quad + E_h - E_h^{***} - E_h^{***}\ln\frac{E_h}{E_h^{***}} + I_u - I_u^{***} - I_u^{***}\ln\frac{I_u}{I_u^{***}} + I_d - I_d^{***} - I_d^{***}\ln\frac{I_d}{I_d^{***}}.
\end{aligned}$$

The time derivative of $V(X(t))$ is given by

$$\frac{dV(X(t))}{dt} = \left(1 - \frac{S_A^{***}}{S_A}\right)\frac{dS_A}{dt} + \left(1 - \frac{I_A^{***}}{I_A}\right)\frac{dI_A}{dt} + \left(1 - \frac{S_V^{***}}{S_V}\right)\frac{dS_V}{dt} + \left(1 - \frac{E_V^{***}}{E_V}\right)\frac{dE_V}{dt} + \left(1 - \frac{I_V^{***}}{I_V}\right)\frac{dI_V}{dt} + \left(1 - \frac{S_h^{***}}{S_h}\right)\frac{dS_h}{dt} + \left(1 - \frac{E_h^{***}}{E_h}\right)\frac{dE_h}{dt} + \left(1 - \frac{I_u^{***}}{I_u}\right)\frac{dI_u}{dt} + \left(1 - \frac{I_d^{***}}{I_d}\right)\frac{dI_d}{dt} + \left(1 - \frac{R_h^{***}}{R_h}\right)\frac{dR_h}{dt},$$

$$\frac{dV(X(t))}{dt} = \left(1 - \frac{N_A^{***}}{N_A}\right)\frac{dN_A}{dt} + \left(1 - \frac{N_V^{***}}{N_V}\right)\frac{dN_V}{dt} + \left(1 - \frac{N_h^{***}}{N_h}\right)\frac{dN_h}{dt},$$

$$\frac{dV(X(t))}{dt} = \left(1 - \frac{N_A^{***}}{N_A}\right)\left(r_L N_V\left(1 - \frac{N_A}{k_A}\right) - (\mu_A + r_A)N_A\right) + \left(1 - \frac{N_V^{***}}{N_V}\right)(r_A N_A - \mu_V N_V) + \left(1 - \frac{N_h^{***}}{N_h}\right)(k_1 - \mu N_h - \mu_u I_u - \mu_d I_d).$$

We use the second-order asymptotic Taylor expansion to prove the local stability of the equilibrium point. The formula $\left(1 - \frac{x^*}{x}\right)(f(x) - f(x^*)) = \frac{f'(x^*)}{x}(x - x^*) + o\left((x - x^*)^2\right)$ where $x > 0$ and $x^* > 0$. Now, if $f'(x^*) < 0$, then: $\left(1 - \frac{x}{x^*}\right)(f(x) - f(x^*)) \leq 0$.

Therefore, $\left(1 - \frac{N_A^{***}}{N_A}\right)\left(r_L N_V\left(1 - \frac{N_A}{k_A}\right) - (\mu_A + r_A)N_A\right) \leq 0$; $\left(1 - \frac{N_V^{***}}{N_V}\right)(r_A N_A - \mu_V N_V) \leq 0$; and $\left(1 - \frac{N_h^{***}}{N_h}\right)(k_1 - \mu N_h - \mu_u I_u - \mu_d I_d) \leq 0$.

We deduce that $\dot{V}(X(t)) \leq 0$, which shows that it is a Lyapunov function.

Moreover, $\dot{V}(X(t)) = 0$ if and only if $S_A = S_A^{***}$,$I_A = I_A^{***}$, $S_V = S_V^{***}$, $E_V = E_V^{***}$, $I_V = I_V^{***}$, $S_h = S_h^{***}$, $E_h = E_h^{***}$, $I_u = I_u^{***}$, $I_d = I_d^{***}$, and $R_h = R_h^{***}$.

According to LaSalle's invariance theorem, the endemic equilibrium point $\mathcal{E}^{***}$ is globally asymptotically stable.

4.3. Parameters estimation

The objective is to estimate the parameters of the model by fitting its outputs to the observed data. We use a set of M observations of the weekly reported new cases, denoted by $I_{w,\text{obs}}(j)$, recorded at times t_j, $j = 1, \ldots, M$. The model prediction for the weekly new cases is given by

$$I_w(t; U) = \beta\, \delta\, E_h(t; U),$$

where $U = (\beta_{mh}, \beta_{hm}, \beta, b, r_L, \alpha_V)$ is the vector of parameters to be estimated (defined in Table 2).

In this equation, $E_h(t; U)$ denotes the number of exposed individuals (compartment E_h) at time t for a given set of parameters U, obtained as the solution of System (3.1).

For the problem in System (3.1), we associate the following definition with the functional J:

$$J(U) = \int_{t_i}^{t_f} \left(I_w(t; U) - I_{w,\text{obs}}(t)\right)^2 dt, \tag{4.2}$$

where t_i and t_f denote the initial and final times, respectively.

The parameter estimation problem consists of solving:

$$\min_{U \subset \mathcal{D}} J(U), \tag{4.3}$$

where $\mathcal{D} = [0, 1]^6$ is a bounded subset of $\mathbb{R}^6$.

Theorem 4.3. *The problem defined by* (3.1) *admits a unique solution, denoted by*

$$U^* = (\beta^*_{mh}, \beta^*_{hm}, \beta^*, b^*, r^*_L, \alpha^*_V).$$

where each component corresponds to the estimated optimal value of the model parameters that best reproduce the observed epidemic dynamics (see Table 2 for a complete description of each parameter).

Thus, U^* represents the set of biological parameters that best capture the observed dynamics of the epidemic.

Proof. Let us define the mapping

$$\mathcal{B} : \mathcal{D} \to L^2(t_i, t_f), \quad U \mapsto Y_U(t),$$

where $Y_U(t)$ is the unique solution of System (3.1) for a given U. We also define

$$\mathcal{H} : L^2(t_i, t_f) \to \mathbb{R}, \quad Y_U(t) \mapsto \int_{t_i}^{t_f} (I_w(t; U) - I_{w,\text{obs}}(t))^2 \, dt.$$

Hence, the functional can be written as a composition:

$$J(U) = \mathcal{H}(I_w(\cdot; U)).$$

The mapping $\mathcal{B}$ is continuous, and $\mathcal{H}$ is quadratic and continuous. Therefore, J is continuous on the compact domain $\mathcal{D} = [0, 1]^6$. By Weierstrass' theorem, J admits at least one minimizer U^*.

If, in addition, the functional J is convex, this minimizer is unique. We then denote it by

$$U^* = (\beta^*_{mh}, \beta^*_{hm}, \beta^*, b^*, r^*_L, \alpha^*_V).$$

5. Presentation of the African vulture optimization algorithm (AVOA)

In this study, the epidemiological parameters of the dengue transmission model were estimated using the African vulture optimization algorithm (AVOA) [18]. This algorithm is a bio-inspired metaheuristic based on the foraging behavior of African vultures, which alternates between global exploration and local exploitation phases to converge toward the optimal solutions.
The steps of the AVOA are shown below.

- Phase 1: Population grouping
  After generating the population, the algorithm divides it into two groups: The first group is led by the best vulture, and the second by the second-best. The vultures are directed toward one another according to a calculated probability.

$$R(i) = \begin{cases} BestVulture_1 & \text{if } p_i = L_1 \\ BestVulture_2 & \text{if } p_i = L_2 \end{cases} \quad \text{for } i = 1, \ldots, N. \tag{5.1}$$

- Phase 2: Rate of starvation of vultures F
  The algorithm calculates the hunger rate of each vulture to determine whether it should explore or exploit the search space.

$$F = (2 \times rand_1 + 1) \times z \times \left(1 - \frac{\text{iteration}_i}{\text{maxiterations}}\right) + t, \tag{5.2}$$

  where
  rand_1: A random value between 0 and 1,
  z: A random value in the interval $[-1, 1]$ that changes at each iteration,

$$t = h \times \left(\sin\left(\omega \frac{\pi}{2} \frac{\text{iteration}_i}{\text{maxiterations}}\right) + \cos\left(\frac{\pi}{2} \frac{\text{iteration}_i}{\text{maxiterations}}\right) - 1 \right),$$

  where
  h: A random number in $[-2, 2]$,
  ω: A constant controlling the exploration phase.
- Phase 3: Exploration
  If $|F| > 1$ (the vulture is hungry), the vulture is in the exploration phase. It adopts one of two random strategies: Either it moves toward a leader or it performs a random search in the solution space.

$$P(i+1) = R(i) - D(i) \times F \tag{5.3}$$

$$P(i+1) = R(i) - F + \text{rand2} \times ((ub - lb) \times \text{rand3} + lb) \tag{5.4}$$

- Phase 4: Exploitation phase (first step)
  The vulture performs a rotational flight around the target or a slow siege attack around the best solution if $0.5 \leq |F| \leq 1$.

$$P(i+1) = D(i) \times (F + \text{rand}_4) - d(t), \quad i = 1, \ldots, N. \tag{5.5}$$

$$P(i+1) = R(i) - (S_1(i) + S_2(i)), \quad i = 1, \ldots, N. \tag{5.6}$$

- Phase 5: Exploitation phase (second step)
  If the vulture is slightly hungry ($|F| < 0.5$), it either gathers around the best vultures or engages in aggressive fighting with Lévy flight to refine the search.

$$P(i+1) = \begin{cases} \text{Eq (5.8)} & \text{if } P_3 \geq \text{rand}_{p3} \\ \text{Eq (5.9)} & \text{if } P_3 < \text{rand}_{p3} \end{cases}, \quad i = 1, \ldots, N. \tag{5.7}$$

$$P(i+1) = \frac{A_1(i) + A_2(i)}{2}, \quad i = 1, \ldots, N. \tag{5.8}$$

$$P(i+1) = R(i) - d(i) \times F \times \text{Levy}(d), \quad i = 1, \ldots, N. \tag{5.9}$$

The pseudo-code of the AVOA is described in Algorithm 1.

Algorithm 1 AVOA for the parameter estimation problem [19].

Inputs: Population dimension N and maximum number of iterations T
Outputs: The location of vulture and its fitness value
Initialize the random population $P_i(i = 1, 2, \ldots, N)$
while stopping condition is not met **do**
  Solve the direct problem (3.1)
  Calculate the fitness values of vulture using the cost function (4.2)
  Set $P_{\text{BestVulture}_1}$ to represent the vulture's position (best position for vulture Category 1)
  Set $P_{\text{BestVulture}_2}$ to represent the vulture's position (second best location best vulture Category 2)
  for each vulture P_i **do**
    Select $R(i)$ according to Eq (5.1)
    Update F according to Eq (5.2)
    if $|F| \geq 1$ **then**
      if $P_1 < \text{rand}_{P_1}$ **then**
        Update the location of vulture via Eq (5.3)
      else
        Update the location of vulture via Eq (5.4)
      end if
    else if $|F| < 1$ **then**
      if $|F| \geq 0.5$ **then**
        if $P_2 < \text{rand}_{P_2}$ **then**
          Update the location of vulture via Eq (5.5)
        else
          Update the location of vulture via Eq (5.6)
        end if
      else
        if $P_3 \geq \text{rand}_{P_3}$ **then**
          Update the location of vulture via Eq (5.8)
        else
          Update the location of vulture via Eq (5.9)
        end if
      end if
    end if
  end for
end while
return $P_{\text{BestVulture}_1}$

6. Results and discussion

6.1. Results of parameters estimation

The data used in this study consist of weekly reported dengue cases from June to December 2023 in the central region of Burkina Faso.

Although the data are weekly, the model was numerically solved using the fourth-order Runge–Kutta (RK4) method with a daily time step. This choice was made to account for the biological and epidemiological realities of the disease. Specifically, the intrinsic incubation period in the human host ranges from approximately 4 to 10 days, whereas the extrinsic incubation period in the *Aedes* vector (the time required for the mosquito to become infectious after biting a viremic host) ranges from about 8 to 12 days [20]. A weekly time unit would not allow for accurate representation of these critical durations.

Similarly, the average lifespan of an adult mosquito is 2–4 weeks, but mortality risk is a daily event. Consequently, the vector mortality rate (μ_V) is defined in nearly all of the literature as a *daily* rate [21]. Moreover, the aquatic developmental cycle (egg, larva, pupa) also unfolds over several days.

Table 3. Parameters related to human and vector dynamics.

Parameters	Range	Values	References
λ	$\approx 9.58904 \times 10^{-5}$	9.58904×10^{-5} day^{-1}	[22, 23]
μ	$\approx 2.19178 \times 10^{-5}$	2.19178×10^{-5} day^{-1}	[22, 23]
k_A	-	9.74322×10^{6}	-
μ_A	[0.05, 0.25]	0.15 day^{-1}	[24, 25]
r_A	[0.07, 0.14]	0.1 day^{-1}	[25]
μ_V	[0.3, 0.13]	0.047619 day^{-1}	[26, 27]
σ_V	[0.083, 0.125]	0.125 day^{-1}	[28]
N_h	-	3.24774×10^{6}	[29]
δ	[0.1, 0.25]	0.166667 day^{-1}	[30, 31]
μ_u	$[1.4 \times 10^{-4}, 1.4 \times 10^{-3}]$	0,001 day^{-1}	[30]
γ_u	[0.14, 0.2]	0.142857 day^{-1}	[30, 31]
μ_d	$> 1.4 \times 10^{-4}$	0.002 day^{-1}	[30]
γ_d	[0.1, 0.2]	0.1 day^{-1}	Assumed

Table 4. Initial conditions used for the model simulation.

Variable	Initial value	Unit
$S_h(0)$	3,212,760	Individuals
$E_h(0)$	2148.25	Individuals
$I_u(0)$	36	Individuals
$I_d(0)$	322.042	Individuals
$R_h(0)$	32,477.4	Individuals
$S_V(0)$	6,495,480	Mosquitoes
$E_V(0)$	10,000	Mosquitoes
$I_V(0)$	100.154	Mosquitoes
$S_A(0)$	3,247,740	Mosquitoes
$I_A(0)$	324.774	Mosquitoes
$N_h(0)$	3,247,740	Individuals

This daily step approach also allows for the simulation of control strategies with high temporal flexibility (e.g., a 10-day spraying campaign), which would be impossible to represent with a weekly

time unit. For calibration purposes, the model's daily outputs were aggregated into weekly data for comparison with the observed cases, ensuring consistency between simulation and estimation.

The fixed parameter values used in the estimation are presented in Table 3. The initial values used are presented in Table 4. Table 5 presents the results of the parameter estimation problem using the AVOA algorithm.

Table 5. Estimated values of the model parameters, with variation ranges and references.

Parameter	Range	Estimated value	Unit/note	References
β_{mh}	[0, 0.5]	0.284499	Probability	[26]
β_{hm}	[0, 0.75]	0.16289	Probability	[26]
β	[0.1, 0.4]	0.100547	Proportion	[32]
b	[0.26, 0.67]	0.400259	Bites/day	[26, 30]
r_L	[4, 10]	6.17254	Day^{-1}	[25]
α_V	[0, 0.11]	0.100074	Proportion	[33, 34]

Figure 2 presents both the observed and the estimated data, demonstrating the robustness of the AVOA algorithm.

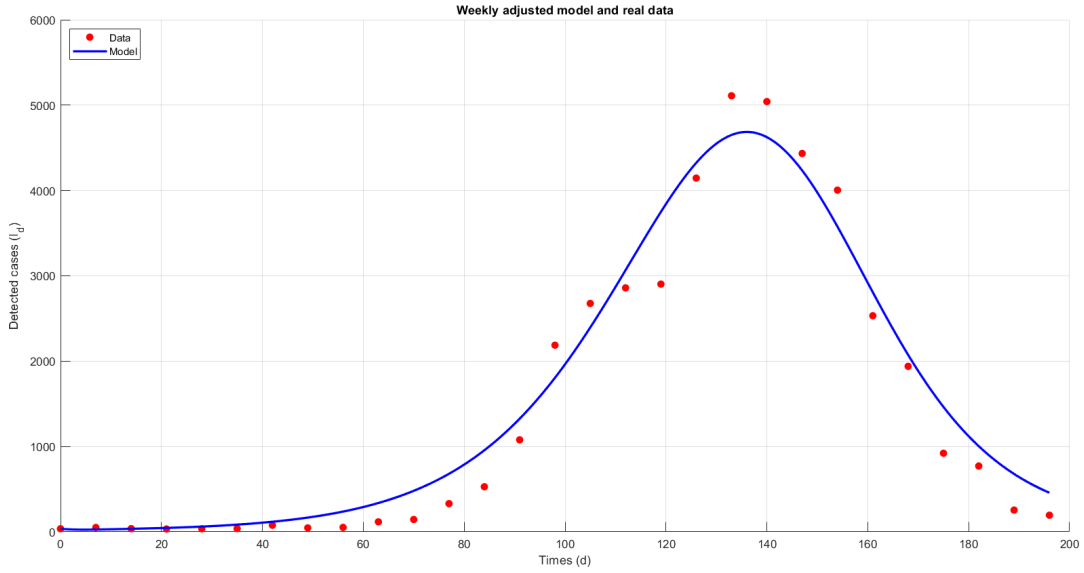

Figure 2. Weekly evolution of dengue cases in Burkina Faso and fit of the proposed model (June–December 2023).

Figure 2 illustrates a satisfactory fit between the mathematical model and the weekly dengue case data recorded in Burkina Faso from June to December 2023. Thanks to the AVOA algorithm, the model parameters were robustly estimated, allowing faithful reproduction of the observed dynamics, notably the rise, peak, and decline of the epidemic. These results demonstrate the relevance of the fitting method used. To assess the influence of parameters on the model's behavior, a sensitivity analysis is presented in the following section.

6.2. Sensitivity analysis

Sensitivity analysis is a fundamental tool for evaluating the influence of the parameters in a complex dynamic model on the basic reproduction number $\mathcal{R}_0$, which determines the endemic threshold. It helps to assess the impact of each parameter on this threshold.

In this study, we used a numerical differentiation approach to calculate the sensitivity indices of $\mathcal{R}_0$ with respect to each model parameter, using the following formula:

$$\chi_{\Upsilon}^{\mathcal{R}_0} = \frac{\partial \mathcal{R}_0}{\partial \Upsilon} \times \frac{\Upsilon}{\mathcal{R}_0}, \tag{6.1}$$

where Υ is a parameter of the model. A positive sensitivity index indicates that an increase in the parameter leads to an increase in $\mathcal{R}_0$, while a negative index suggests that it decreases $\mathcal{R}_0$. The parameters were estimated using the African vulture optimization algorithm (AVOA), based on dengue case data in Burkina Faso. Table 6 provides the numerical values of the sensitivity indices.

Table 6. Sensitivity indices of the model parameters.

Sensitivity index	Values
$\chi_{\mu_A}^{R_0} = \left(\frac{\partial R_0}{\partial \mu_A}\right) \times \left(\frac{\mu_A}{R_0}\right)$	−0.005768
$\chi_{r_A}^{R_0} = \left(\frac{\partial R_0}{\partial r_A}\right) \times \left(\frac{r_A}{R_0}\right)$	0.494635
$\chi_{\mu_V}^{R_0} = \left(\frac{\partial R_0}{\partial \mu_V}\right) \times \left(\frac{\mu_V}{R_0}\right)$	−1.122208
$\chi_{\sigma_V}^{R_0} = \left(\frac{\partial R_0}{\partial \sigma_V}\right) \times \left(\frac{\sigma_V}{R_0}\right)$	0.134860
$\chi_{\delta}^{R_0} = \left(\frac{\partial R_0}{\partial \delta}\right) \times \left(\frac{\delta}{R_0}\right)$	0.000064
$\chi_{\gamma_N}^{R_0} = \left(\frac{\partial R_0}{\partial \gamma_N}\right) \times \left(\frac{\gamma_N}{R_0}\right)$	−0.419293
$\chi_{\gamma_h}^{R_0} = \left(\frac{\partial R_0}{\partial \gamma_h}\right) \times \left(\frac{\gamma_h}{R_0}\right)$	−0.065255
$\chi_{r_L}^{R_0} = \left(\frac{\partial R_0}{\partial r_L}\right) \times \left(\frac{r_L}{R_0}\right)$	0.009614
$\chi_{\alpha_V}^{R_0} = \left(\frac{\partial R_0}{\partial \alpha_V}\right) \times \left(\frac{\alpha_V}{R_0}\right)$	0.022266
$\chi_{k_A}^{R_0} = \left(\frac{\partial R_0}{\partial k_A}\right) \times \left(\frac{k_A}{R_0}\right)$	0.488761
$\chi_{b}^{R_0} = \left(\frac{\partial R_0}{\partial b}\right) \times \left(\frac{b}{R_0}\right)$	0.977734
$\chi_{\beta_{mh}}^{R_0} = \left(\frac{\partial R_0}{\partial \beta_{mh}}\right) \times \left(\frac{\beta_{mh}}{R_0}\right)$	0.488867
$\chi_{\beta_{hm}}^{R_0} = \left(\frac{\partial R_0}{\partial \beta_{hm}}\right) \times \left(\frac{\beta_{hm}}{R_0}\right)$	0.488867
$\chi_{\beta}^{R_0} = \left(\frac{\partial R_0}{\partial \beta}\right) \times \left(\frac{\beta}{R_0}\right)$	0.019368

Figure 3 highlights the impact of each parameter on the endemic threshold. The analysis shows parameters in the following categories.

- **Positive sensitivity values** are:

$$\chi_{r_A}^{R_0} = 0.494635, \quad \chi_{\sigma_V}^{R_0} = 0.134860, \quad \chi_{\delta}^{R_0} = 0.000064, \quad \chi_{r_L}^{R_0} = 0.009614, \quad \chi_{\alpha_V}^{R_0} = 0.022266,$$

$$\chi_{k_A}^{R_0} = 0.488761, \quad \chi_{b}^{R_0} = 0.977734, \quad \chi_{\beta_{mh}}^{R_0} = 0.488867, \quad \chi_{\beta_{hm}}^{R_0} = 0.488867, \quad \chi_{\beta}^{R_0} = 0.019368.$$

The parameters $r_A, \sigma_V, \delta, r_L, \alpha_V, k_A, b, \beta_{mh}, \beta_{hm}$, and β contribute to increasing the value of $\mathcal{R}_0$. The analysis emphasizes that to effectively contain the disease's spread, it is essential to reduce contacts

between humans and mosquitoes by targeting the biting rate b and the transmission probabilities β_{mh} and β_{hm}. It is also necessary to limit the vector's reproduction and development by controlling the maturation rate r_A and the larval carrying capacity k_A. These highly influential parameters represent strategic targets for lowering $\mathcal{R}_0$ below the endemic threshold.

- **Negative sensitivity values** are:

$$\chi_{\mu_A}^{R_0} = -0.005768, \quad \chi_{\mu_V}^{R_0} = -1.122208, \quad \chi_{\gamma_N}^{R_0} = -0.419293, \quad \chi_{\gamma_h}^{R_0} = -0.065255.$$

The parameters μ_A, μ_V, γ_N, and γ_h contribute to decreasing the value of $\mathcal{R}_0$. The analysis reveals that the adult mosquito mortality rate μ_V and the recovery rate of undetected infected humans γ_N are the most influential parameters with negative sensitivity. This highlights the effectiveness of strategies aimed at reducing the lifespan of adult mosquitoes (such as insecticide use and destruction of larval breeding sites) on the one hand, and approaches that promote recovery of undetected infected individuals by facilitating rapid care and raising awareness of preventive behaviors on the other hand.

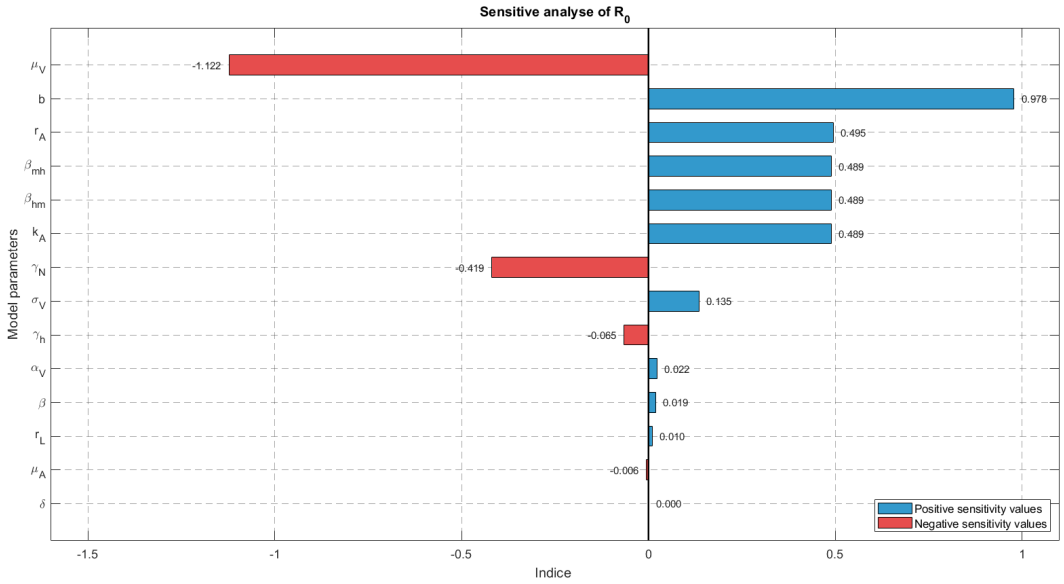

Figure 3. Sensitivity indices of the model parameters.

7. Simulation of dengue control strategies

The dynamics of the *Aedes aegypti* mosquito play a crucial role in dengue transmission. To contain the disease, various control strategies can be implemented. This section evaluates the impact of three major interventions: Limiting larval breeding sites, increasing adult mosquito mortality, and reducing the biting rate. These interventions are analyzed individually and in combination over periods of 4 and 8 weeks to identify the most effective and sustainable approaches. The baseline simulation without intervention shows an epidemic peak of 328,282 cases on Day 141.9.

7.1. Impact of larval source reduction

Reducing mosquito breeding sites, simulated through a 10%, 25%, and 50% decrease in the larval carrying capacity (k_A), leads to a substantial decline in case numbers and a delay in the epidemic peak (Figure 4). For these reduction levels, the epidemic peak is lowered to 300,392 (Day 150), 253,075 (Day 166), and 154,330 (Day 214) cases. This intervention results in a total case reduction ranging from 2.2% to 56.2% and causes the basic reproduction number ($\mathcal{R}_0$) to decrease from 2.30 to 1.6. By limiting the adult mosquito population, this strategy effectively flattens and delays the epidemic curve, significantly slowing down transmission.

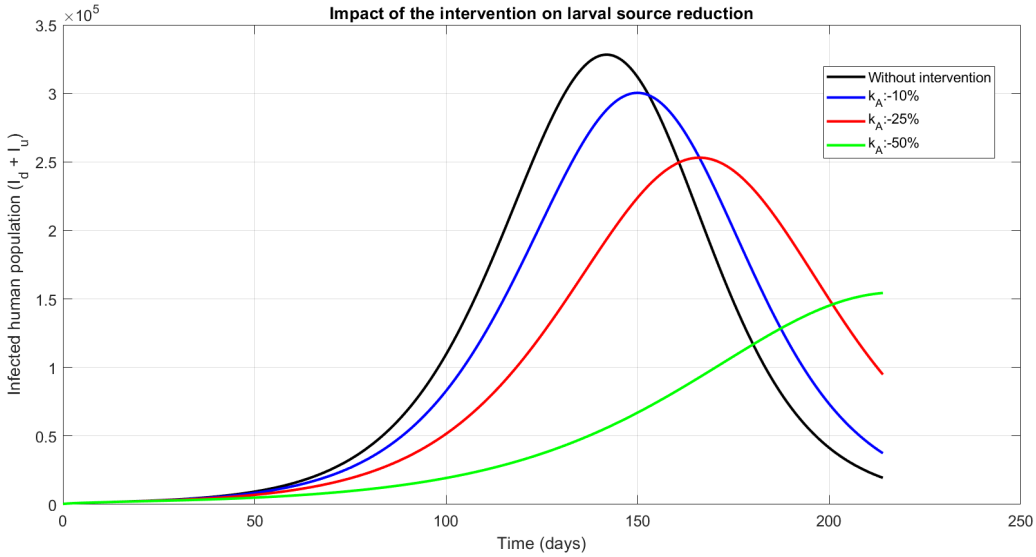

Figure 4. Impact of reducing larval sources.

7.2. Impact of increasing adult mosquito mortality

Increasing adult mosquito mortality (μ_V) is a key vector control strategy aimed at reducing mosquitoes lifespan and transmission capacity. We simulated the effect of increasing μ_V by 50%, 100%, and 200% for durations of 4 and 8 weeks.

A 4-week intervention (Figure 5) delayed the epidemic's peak but had a limited impact on its magnitude, with transmission resurging shortly after the measures were lifted. The effectiveness, measured as total case reduction, ranged from 2.7% to 45.7%.

In contrast, extending the intervention to 8 weeks (Figure 6) yielded a substantially greater and more sustained effect. For instance, a 200% increase in μ_V lowered the peak to 172,499 cases and delayed it to Day 214. The effectiveness of this scenario increased significantly, ranging from 9.1% to 77.6%, highlighting the critical importance of the intervention's duration.

This strategy profoundly impacts the basic reproduction number ($\mathcal{R}_0$), which dropped from a baseline of 2.30 to as low as 0.6. This indicates that an intense and prolonged adulticidal intervention can suppress transmission below the epidemic threshold.

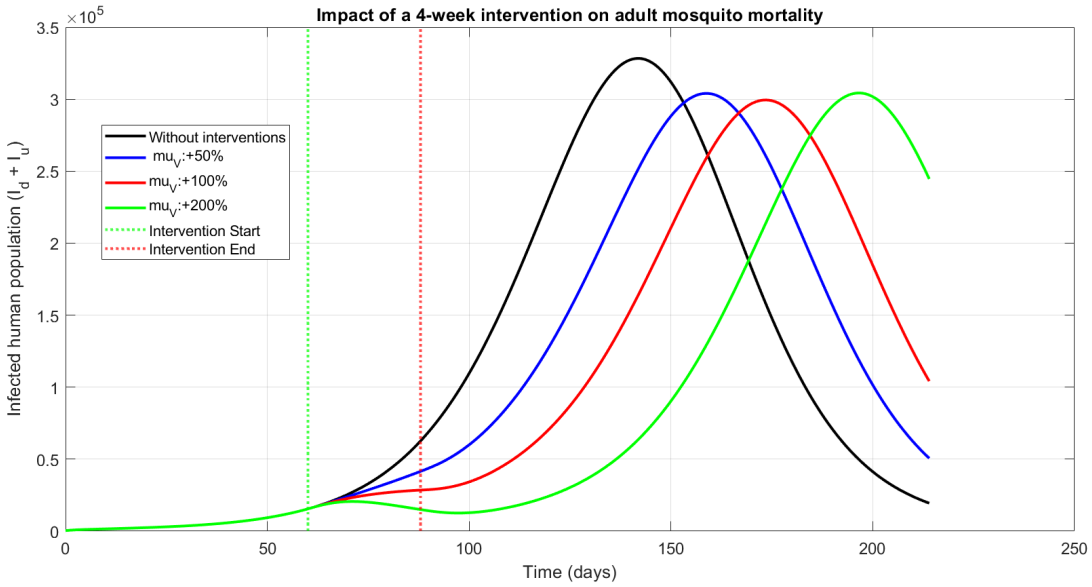

Figure 5. Impact of increasing adult mosquito mortality: 4-week intervention.

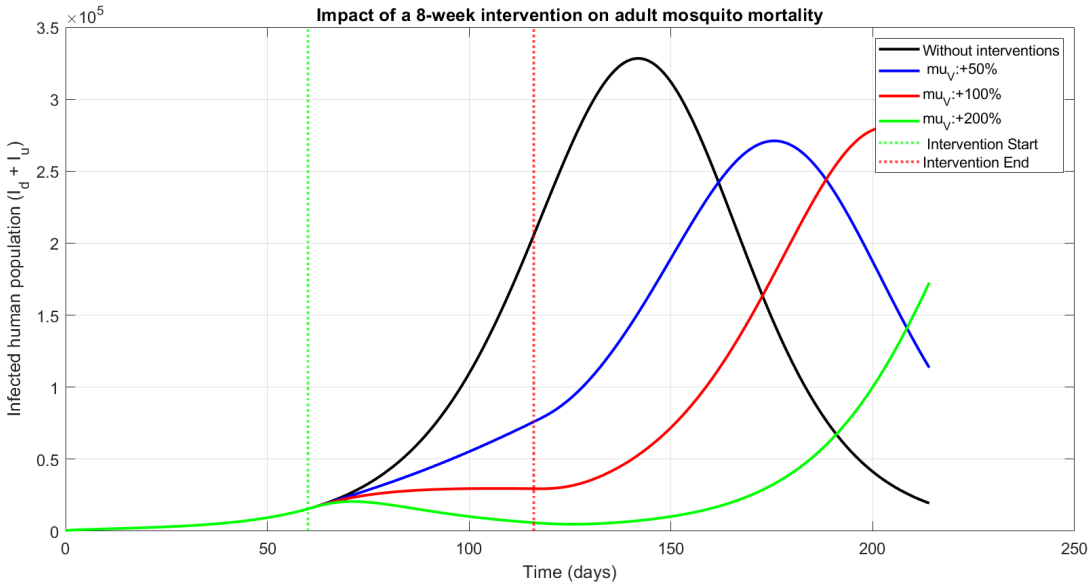

Figure 6. Impact of increasing adult mosquito mortality: 8-week intervention.

7.3. Impact of reducing the biting rate

Reducing the mosquito biting rate (b) is a crucial strategy for limiting vector–human contact and mitigating the epidemic's spread. Our simulations, which reduced this rate by 10%, 20%, and 30%, demonstrate a substantial impact on the epidemic's trajectory (Figure 7).

The strategy effectively flattens and delays the epidemic curve. A 10% reduction lowers the peak to 274,696 cases (Day 161.9), while a 30% reduction dramatically suppresses it to 136,824 cases (Day 214). This corresponds to a cumulative case reduction ranging from 6.8% to 68.7%.

This effect is reflected in the basic reproduction number ($\mathcal{R}_0$), which drops from a baseline of 2.30 to 1.6 under a 30% reduction scenario. These findings highlight the efficacy of public health campaigns in promoting individual protection measures, such as using mosquito nets and repellents, which directly contribute to reducing the biting rate.

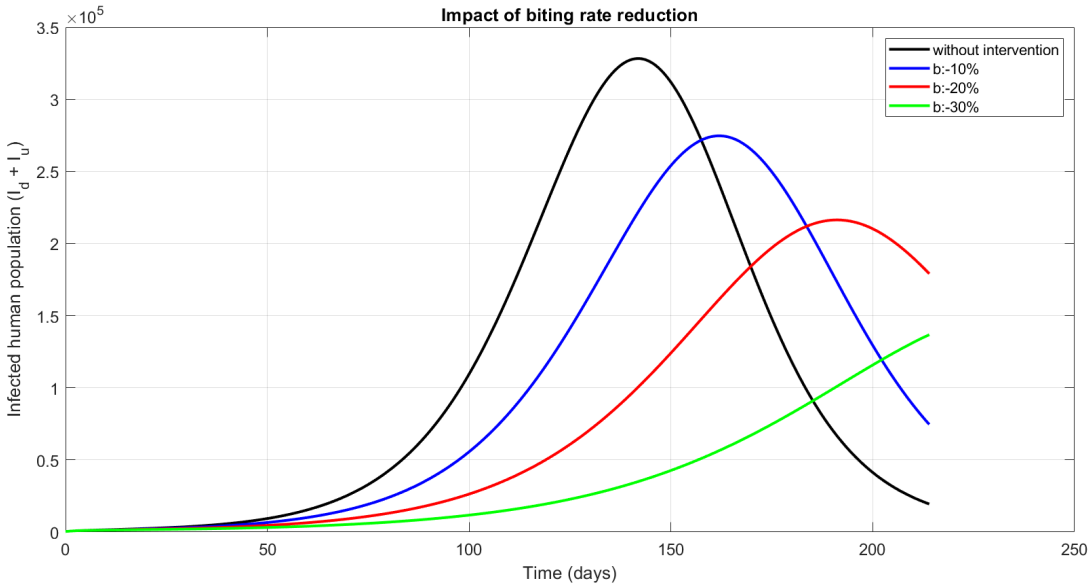

Figure 7. Impact of increasing adult mosquito mortality.

7.4. Larval reduction and increased adult mortality (k_A and μ_V)

Combining a reduction in larval sites (decreased k_A) with increased adult mosquito mortality (increased μ_V) yields a powerful synergistic effect in controlling the epidemic.

While a 4-week intervention (Figure 8) shows significant impact, its durability is limited. Under the highest intensity scenario (a 50% reduction in k_A and a 200% increase in μ_V), the epidemic's peak was reduced to just 33,418 cases, and subsequent resurgence was slow. However, for lower-intensity interventions, transmission rebounded quickly after the measures were lifted. The overall reduction in total cases for this duration ranged from 7.3% to 93.0%.

Extending the intervention to 8 weeks (Figure 9) amplifies this effect, leading to a more pronounced and sustained control. In the highest-intensity scenario, the epidemic is virtually eradicated, with the peak plummeting to only 7217 cases. This corresponds to a cumulative case reduction of 97.6%, compared with 17.7% for the mildest intervention.

This integrated approach dramatically reduces the basic reproduction number ($\mathcal{R}_0$) from a baseline of 2.3 to as low as 0.5. These results underscore the critical importance of a prolonged, integrated strategy that targets both larval and adult vector stages to achieve near-elimination of transmission.

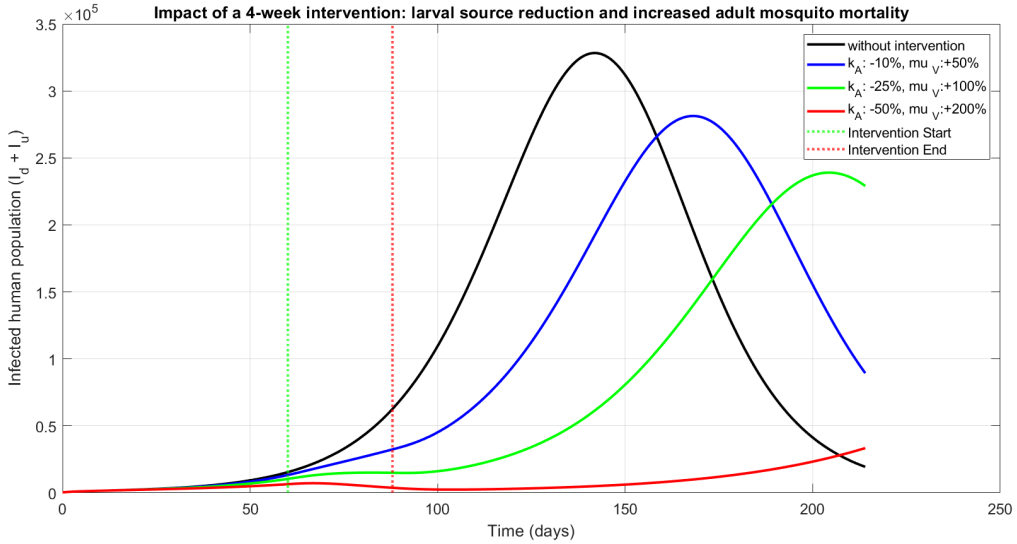

Figure 8. Four-week combined impact: Larval reduction and increased adult mosquito mortality.

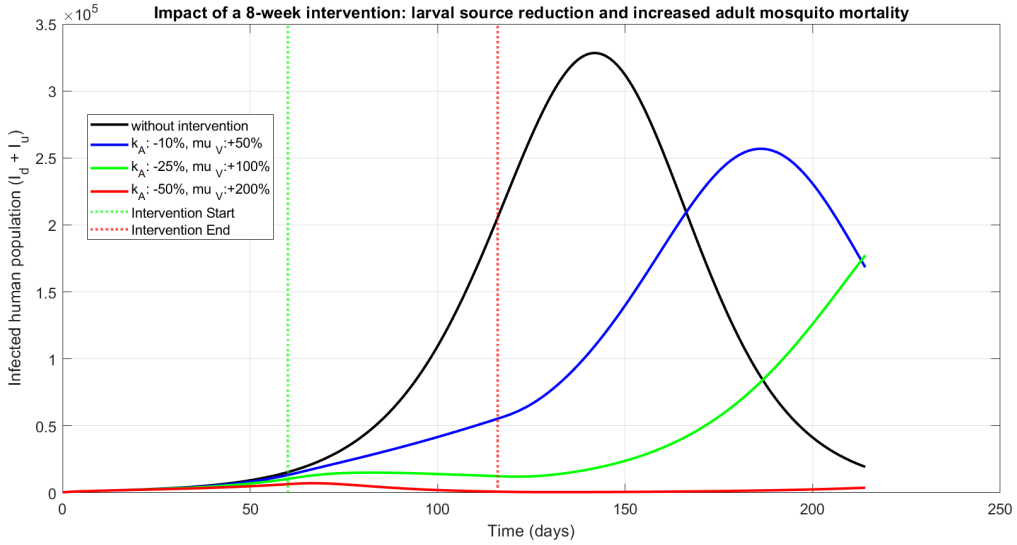

Figure 9. Eight-week combined impact: Larval reduction and increased adult mosquito mortality.

7.5. Increased adult mortality and reduced biting rate (μ_V and b)

A synergistic strategy that combines increased adult mosquito mortality (μ_V) with a reduced biting rate (b) demonstrates exceptional efficacy in controlling dengue's transmission (Figures 10 and 11).

A 4-week intervention significantly reduces the epidemic's transmission. For instance, while a mild intervention (+50% μ_V, −10% b) lowers the peak to 261,413 cases, the most aggressive scenario (+200% μ_V, −30% b) slashes the peak to just 20,293 cases. This corresponds to a total case reduction ranging from 16.4% to 95.7%.

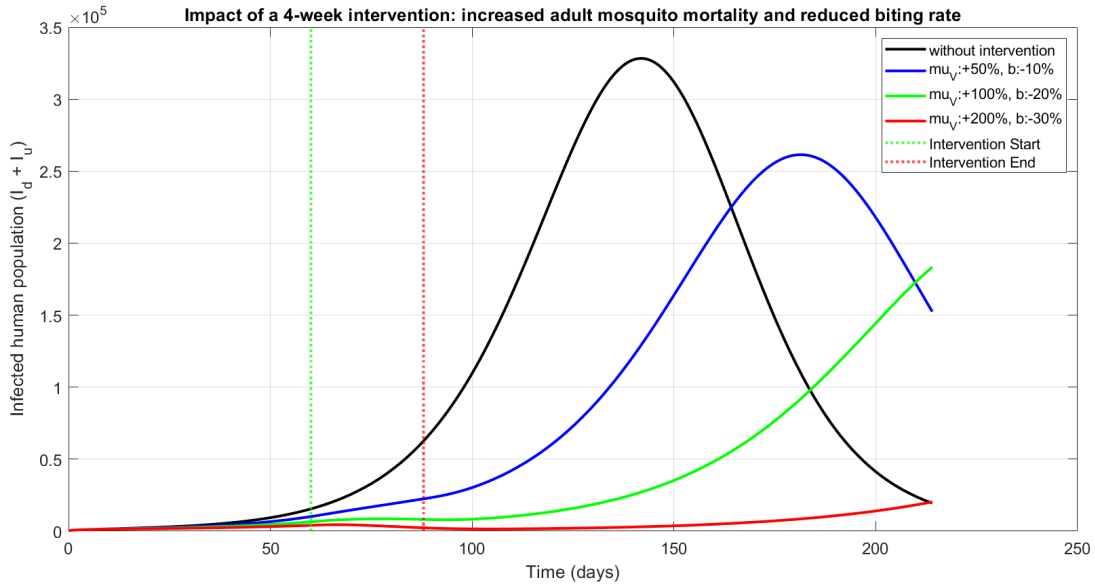

Figure 10. Four-week intervention: Increasing adult mosquito mortality and reducing biting rate.

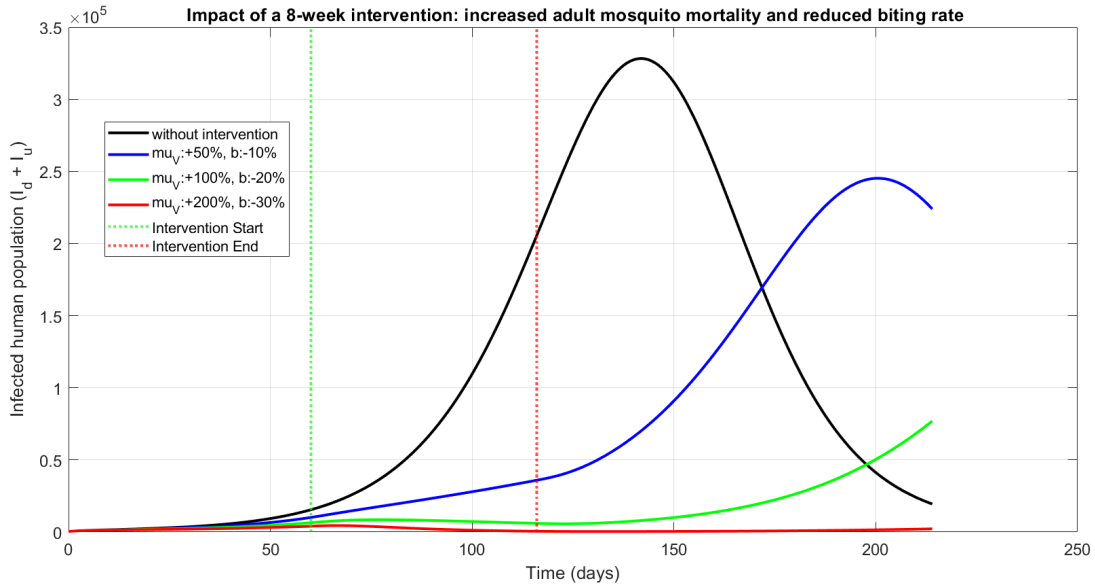

Figure 11. Eight-week intervention: Increasing adult mosquito mortality and reducing biting rate.

Extending the intervention to eight weeks results in near-elimination levels of control. The highest-intensity combination virtually flattens the curve, with the peak reduced to a mere 4481 cases and a cumulative case reduction of 98.5%. This profound impact is reflected in the basic reproduction number ($\mathcal{R}_0$), which plummets from 2.3 to 0.5, well below the epidemic threshold.

These findings underscore that a sustained, dual-action approach simultaneously shortening the

vector's lifespan and minimizing vector–host contact is a powerful strategy for halting the epidemic's spread.

7.6. Combination of the three strategies (k_A, μ_V, and b)

A comprehensive strategy integrating all three interventions (larval site reduction (k_A), increased adult mortality (μ_V), and reduced biting rate (b)) demonstrates unparalleled efficacy in controlling the epidemic.

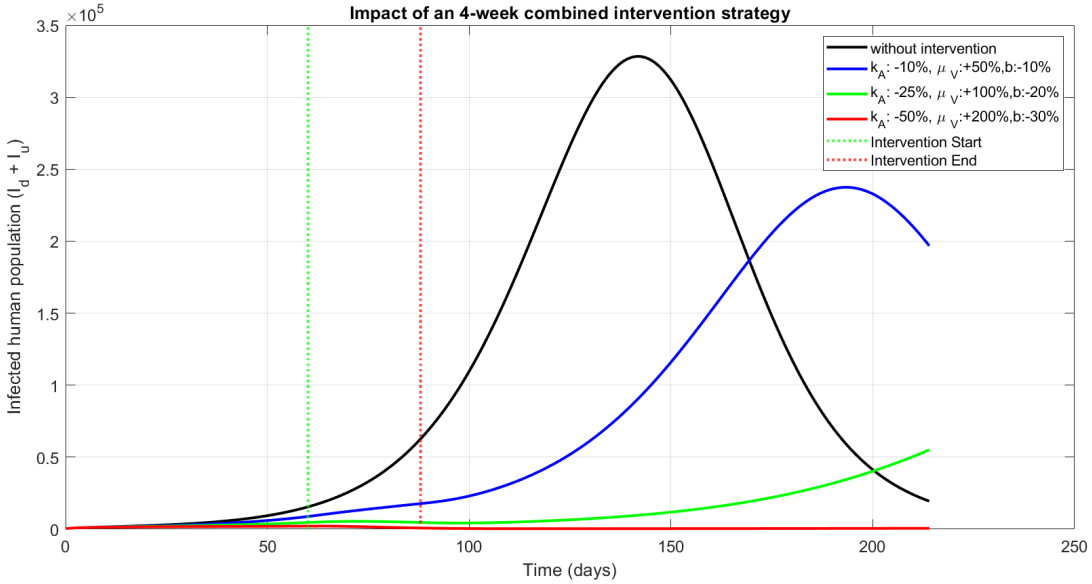

Figure 12. Four-week combined intervention: Impact of the combined intervention strategy.

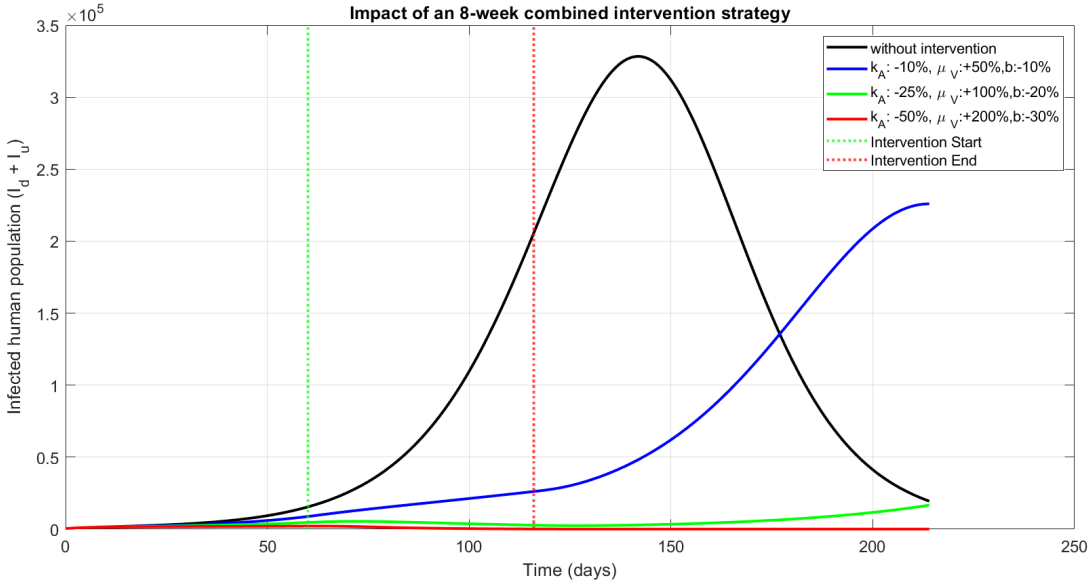

Figure 13. Eight-week combined intervention: Impact of the combined intervention strategy.

A 4-week intervention (Figure 12) shows a remarkable dose-dependent impact. While the mildest combination of measures reduces the peak to 237,390 cases (28.4% effectiveness), the most aggressive combination nearly flattens the epidemic curve, suppressing the peak to a mere 2131 cases and achieving 99.1% effectiveness in total case reduction.

Extending the intervention to 8 weeks (Figure 13) solidifies this control and ensures its longevity by preventing post-intervention resurgence. In the highest-intensity scenario, the epidemic is decisively halted, with the peak remaining at just 2131 cases and the overall effectiveness reaching 99.3%.

This integrated approach has a profound impact on transmission dynamics, causing the basic reproduction number ($\mathcal{R}_0$) to plummet from a baseline of 2.3 to an extremely low 0.3. These findings highlight that a sustained, multi-faceted strategy that simultaneously targets larval, adult, and behavioral components of the transmission cycle is the most robust path toward elimination of the epidemic.

7.7. General conclusion on control strategies

The simulations consistently demonstrate that the effectiveness of dengue control strategies strongly depends on their intensity and, especially, their duration.

- Four-week interventions have a temporary impact: They delay and reduce the epidemic's peak but are insufficient to prevent a rapid resurgence of transmission.
- Eight-week interventions are significantly more effective, leading to sustained epidemic control, and even local elimination in the most intensive scenarios.
- Combined strategies consistently outperform single interventions, with the combination of all three measures (larval control, adulticide, and biting rate reduction) yielding the best results.

These findings highlight the necessity of implementing integrated, intensive, and prolonged vector control actions to sustainably manage the transmission of dengue.

8. Conclusions

In this study, we developed a compartmental model to analyze dengue's transmission dynamics in Burkina Faso. Our approach combines three frameworks: Susceptible-infected (SI) for the aquatic phase of mosquitoes, susceptible-exposed-infected (SEI) for the vector population, and susceptible-exposed-infected-recovered (SEIR) for the human population. The model incorporates vertical transmission in mosquitoes, a feature that has been seldom explored in previous research.

Parameter estimation was performed using the African vulture optimization algorithm (AVOA), enabling the quantification of key unknown parameters. A subsequent sensitivity analysis identified the most influential drivers of dengue transmission, including mosquito biting rate, transmission probabilities, and several vector life-cycle parameters. Adult mosquito mortality and the recovery rate of undetected cases were also shown to be critical factors for limiting disease spread.

Numerical simulations demonstrated that strategies combining larval source reduction, increased adult mosquito mortality, and reduced biting rates are highly effective for epidemic control. According to our model, these simultaneous interventions can reduce the basic reproduction number ($\mathcal{R}_0$) from 2.3 to 0.3, resulting in a sharp decline in case numbers. Furthermore, maintaining these measures for at least eight weeks, together with public awareness campaigns, is essential for achieving sustainable, long-term control.

Limitations and perspectives: Several limitations should be noted. Our model assumes a single dominant serotype, does not account for climatic factors affecting mosquito population, and does not include analyses of the cost-effectiveness of the interventions. Future work should focus on collecting serotype-specific data and conducting entomological surveys to better calibrate the model and optimize control strategies. Incorporating climatic variability and economic analyses will further enhance the operational relevance of the model for public health decision-making.

Use of AI tools declaration

The authors declare they have not used artificial intelligence (AI) tools in the creation of this article.

Conflict of interest

The authors declare there is no conflict of interest.

References

1. *World Health Organization*, *Dengue – Global Situation*, *Disease Outbreak News*, 2023. Available from: https://www.who.int/fr/emergencies/disease-outbreak-news/item/2023-DON498.
2. H. Abboubakar, A. K. Guidzavaï, J. Yangla, I. Damakoa, R. Mouangue, Mathematical modeling and projections of a vector-borne disease with optimal control strategies: A case study of the Chikungunya in Chad, *Chaos, Solitons Fractals*, **150** (2021), 111197. https://doi.org/10.1016/j.chaos.2021.111197
3. M. Arquam, A. Singh, H. Cherifi, Impact of seasonal conditions on vector-borne epidemiological dynamics, *IEEE Access*, **8**, (2020), 2995650. https://doi.org/10.1109/ACCESS.2020.2995650
4. M. A. Khan, Dengue infection modeling and its optimal control analysis in East Java, Indonesia, *Heliyon*, **7** (2021), e06023. https://doi.org/10.1016/j.heliyon.2021.e06023
5. W. Wartono, M. Soleh, Y. Muda, Mathematical model of dengue control with control of mosquito larvae and mosquito affected by climate change, *BAREKENG J. Ilmu Mat. Ter.*, **15** (2021), 417–426. https://doi.org/10.30598/barekengvol15iss3pp417-426
6. P. J. Witbooi, An SEIR model with infected immigrants and recovered emigrants, *Adv. Differ. Equations*, **2021** (2021), 1–15. https://doi.org/10.1186/s13662-021-03488-5
7. P. Pongsumpun, The dynamical model of dengue vertical transmission, *Curr. Appl. Sci. Technol.*, **17** (2017), 48–61.
8. Y. Guo, T. Li, Fractional-order modeling and optimal control of a new online game addiction model based on real data, *Commun. Nonlinear Sci. Numer. Simul.*, **121** (2023), 107221. https://doi.org/10.1016/j.cnsns.2023.107221
9. Y. Guo, T. Li, Modeling the competitive transmission of the Omicron strain and Delta strain of COVID-19, *J. Math. Anal. Appl.*, **526** (2023), 127283. https://doi.org/10.1016/j.jmaa.2023.127283
10. T. Li, Y. Guo, Modeling and optimal control of mutated COVID-19 (Delta strain) with imperfect vaccination, *Chaos, Solitons Fractals*, **156** (2022), 111825. https://doi.org/10.1016/j.chaos.2022.111825

11. L. Zou, J. Chen, X. Feng, S. Ruan, Analysis of a dengue model with vertical transmission and application to the 2014 dengue outbreak in Guangdong Province, China, *Bull. Math. Biol.*, **80** (2018), 2633–2651. https://doi.org/10.1007/s11538-018-0480-9
12. P. M. Luz, C. T. Codeço, E. Massad, C. J. Struchiner, Uncertainties regarding dengue modeling in Rio de Janeiro, Brazil, *Mem. Inst. Oswaldo Cruz*, **98** (2003), 871–878.
13. P. van den Driessche, J. Watmough, Reproduction numbers and sub-threshold endemic equilibria for compartmental models of disease transmission, *Math. Biosci.*, **180** (2002), 29–48. https://doi.org/10.1016/S0025-5564(02)00108-6
14. Y. Dumont, F. Chiroleu, Vector control for the Chikungunya disease, *Math. Biosci. Eng.*, **7** (2010), 313–345. https://doi.org/10.3934/mbe.2010.7.313
15. A. Khan, R. Zarin, I. Ahmed, A. Yusuf, U. W. Humphries, Numerical and theoretical analysis of rabies model under the harmonic mean type incidence rate, *Results Phys.*, **29** (2021), 104652. https://doi.org/10.1016/j.rinp.2021.104652
16. C. Castillo-Chavez, S. Blower, P. van den Driessche, D. Kirschner, A. A. Yakubu, *Mathematical Approaches for Emerging and Reemerging Infectious Diseases: Models, Methods, and Theory*, Springer Science & Business Media, **126** (2002).
17. C. Castillo-Chavez, On the computation of R_0 and its role on global stability, in *Mathematical Approaches for Emerging and Re-emerging Infection Diseases: An Introduction*, **125** (2002), 31–65.
18. B. Abdollahzadeh, F. S. Gharehchopogh, S. Mirjalili, African vultures optimization algorithm: A new nature-inspired metaheuristic algorithm for global optimization problems, *Comput. Ind. Eng.*, **158** (2021), 107408. https://doi.org/10.1016/j.cie.2021.107408
19. H. Tinde, A. Kiemtore, W. O. Sawadogo, P. O. F. Ouedraogo, I. Zangré, Estimation of epidemiological parameters for COVID-19 cases in Burkina Faso using African vulture optimization algorithm (AVOA), *Int. J. Anal. Appl.*, **22** (2024), 203. https://doi.org/10.28924/2291-8639-22-2024-203
20. *World Health Organization*, *Dengue and Severe Dengue*, 2023. Available from: https://www.who.int/news-room/fact-sheets/detail/dengue-and-severe-dengue.
21. M. J. Keeling, P. Rohani, *Modeling Infectious Diseases in Humans and Animals*, Princeton University Press, 2008.
22. C. Rossier, A. Soura, B. Baya, G. Compaoré, B. Dabiré, Profile: The Ouagadougou health and demographic surveillance system, *Int. J. Epidemiol.*, **41** (2012), 658–666. https://doi.org/10.1093/ije/dys090
23. Banque Mondiale, *Espérance de vie à la Naissance, Total (Années) - Burkina Faso*, 2024. Available from: https://donnees.banquemondiale.org/indicateur/SP.DYN.LE00.IN?locations=BF.
24. H. M. Yang, M. L. G. Macoris, K. C. Galvani, M. T. M. Andrighetti, D. M. V. Wanderley, Assessing the effects of temperature on the population of *Aedes aegypti*, the vector of dengue, *Epidemiol. Infect.*, **137** (2009), 1188–1202. https://doi.org/10.1017/S0950268809002040
25. D. A. Focks, D. G. Haile, E. Daniels, G. A. Mount, Dynamic life table model for Aedes aegypti (Diptera: Culicidae): Simulation results and validation, *J. Med. Entomol.*, **30** (1993), 1018–1028. https://doi.org/10.1093/jmedent/30.6.1018

26. M. Aguiar, V. Anam, K. B. Blyuss, C. D. S. Estadilla, B. V. Guerrero, D. Knopoff, et al., Mathematical models for dengue fever epidemiology: A 10-year systematic review, *Phys. Life Rev.*, **40** (2022), 65–92. https://doi.org/10.1016/j.plrev.2022.02.001

27. O. J. Brady, N. Golding, D. M. Pigott, M. U. G. Kraemer, J. P. Messina, R. C. Reiner Jr, et al., Global temperature constraints on Aedes aegypti and Ae. albopictus persistence and competence for dengue virus transmission, *Parasites Vectors*, **7** (2014), 338. https://doi.org/10.1186/1756-3305-7-338

28. *Organisation Mondiale de la Santé (OMS)*, *Dengue et Dengue Sévère*, 2024. Available from: https://www.who.int/fr/news-room/fact-sheets/detail/dengue-and-severe-dengue.

29. *Institut National de la Statistique et de la Démographie (INSD)*, *Volume 4: Projections Démographiques 2020–2035, Recensement Général de la Population et de l'Habitation du Burkina Faso*, INSD, 2023. Available from: https://www.insd.bf/publications.

30. *World Health Organization*, *Dengue: Guidelines for diagnosis, treatment, prevention and control*, 2009. Available from: https://www.who.int/publications/i/item/9789241547871.

31. D. J. Gubler, Dengue and dengue hemorrhagic fever, *Clin. Microbiol. Rev.*, **11** (1998), 480–496. https://doi.org/10.1128/cmr.11.3.480

32. S. Bhatt, P. Gething, O. Brady, J. P. Messina, A. W. Farlow, C. L. Moyes, et al., The global distribution and burden of dengue, *Nature*, **496** (2013), 504–507. https://doi.org/10.1038/nature12060

33. B. Adams, M. Boots, How important is vertical transmission in mosquitoes for the persistence of dengue? Insights from a mathematical model, *Epidemics*, **2** (2010), 1–10. https://doi.org/10.1016/j.epidem.2010.01.001

34. L. Zou, J. Chen, X. Feng, S. Ruan, Analysis of a dengue model with vertical transmission and application to the 2014 dengue outbreak in Guangdong Province, China, *Bull. Math. Biol.*, **80** (2018), 2633–2651. https://doi.org/10.1007/s11538-018-0480-9

AIMS Press